Published in final edited form as:
J Org Chem. 2012 September 21; 77(18): 7804–7814. doi:10.1021/jo3006842.

Catalytic Coupling of Arene C-H Bonds and Alkynes for the Synthesis of Coumarins: the Substrate Scope and Application to the Development of Neuroimaging Agents

Paul A. Vadola and **Dalibor Sames**
Department of Chemistry, Columbia University, 3000 Broadway, New York, New York 10027

Dalibor Sames: sames@chem.columbia.edu

Abstract

C-H bond functionalization offers strategically novel approaches to complex organic compounds, however many C-H functionalization reactions suffer from poor compatibility with Lewis basic functional groups; especially amines, which are often essential for biological activity. This study describes a systematic examination of the substrate scope of catalytic hydroarylation in the context of complex amino coumarin synthesis. The choice of substrates was guided by the design and development of the next generation of Fluorescent False Neurotransmitters (FFNs); neuroimiaging probes we recently introduced for optical imaging of neurotransmission in the brain. Comparison of two mild protocols, using catalytic $PtCl_4$ or $Au(PPh_3)Cl/AgSbF_6$, revealed that each method has a broad and mutually complementary substrate scope. The relatively less active platinum system out-performed the gold catalyst with indole substrates lacking substitution at the C-3 position and provided higher regioselectivity in the case of carbazole-based substrates. On the other hand, the more active gold catalyst demonstrated excellent functional group tolerance, and the ability to catalyze the formation of highly strained, helical products. The development of these two protocols offers enhanced substrate scope and provides versatile synthetic tools required for the structure-activity examination of FFN neuroimaging probes as well as for the synthesis of complex coumarins in general.

Introduction

C-H bond functionalization is an active area of research. Demonstration of novel strategic opportunities in complex organic synthesis afforded by C-H bond functionalization led to a shift of attention from simple hydrocarbons to complex organic substrates containing a diversity of functional groups.[1] Indeed, the field has progressed to such an extent that C-H bond functionalization is widely considered during synthetic planning of diverse organic materials including protein ligands, drug candidates, biological probes and other functional materials. Thus, in addition to the exploration of new reactivity modes (to directly convert C-H bonds to new functionalities or C-C bonds), it is important to expand the scope and practical applicability of the C-H functionalization processes for the field to realize its full impact. Here we describe a remarkably broad substrate scope of the catalytic intramolecular hydroarylation of alkynes and its use in the development of fluorescent neuroimaging probes.

Correspondence to: Dalibor Sames, sames@chem.columbia.edu.

Supporting Information Available: NMR spectra for all substrates and products, and X-ray data for compound **14.** This material is available free of charge via the Internet at http://pubs.acs.org.

Hydroarylation of alkynes defines an overall process of the addition of an arene C-H bond across an alkyne. In an intramolecular manner, this process provides a direct route to valuable organic compounds such as benzo-fused heterocycles and carbocycles (Scheme 1). In contrast to standard cross-coupling methodologies, hydroarylation eliminates the requirement for a functional group on the participating arene ring (halide, psedohalide, boronate) and the power of hydroarylation is realized in its ability to form C-C bonds directly from C-H bonds with absolute atom economy (Scheme 1).[2]

Our laboratories have been pursuing the development hydroarylation reactions, which led to the $PtCl_4$ catalyzed hydroarylation of alkynes affording a wide variety of complex products (Scheme 1, eq. 1).[3] In addition, we developed the ruthenium-catalyzed hydroarylation of alkenes providing rapid access to dihydrobenzofurans and dihydrobenzopyrans.[4] We were interested in the application of the $PtCl_4$ protocol for the cyclization of aryl alkynoate esters as a mild route to complex coumarins (Scheme 1, eq. 2) complementing the relatively harsh conditions of the classical von Pechmann condensation.[5] This project was fueled by our interest in the development of fluorescent reporters for imaging metabolism and neurotransmission in the brain. The coumarins are particularly attractive in this context due to their relatively small molecular size, high brightness and good photostability.

Coumarin-based fluorescent probes for dopamine metabolism and neurotransmission

We have developed a reporter substrate for monoamine oxidases, enzymes involved in metabolism of dopamine and other monoamine neurotransmitters, based on the coumarin nucleus.[6] The dopamine system plays a key role in many fundamental processes of the brain including generation of motivational forces and subjective reward, habit learning, working memory and cognition.[7] Aberrations of dopaminergic neurotransmission have been implicated in numerous neuropsychiatric disorders such as Parkinson's disease, schizophrenia, drug addiction and attention deficit hyperactive disorder (ADHD).[8] It is now widely accepted that learning is dependent on plasticity of synaptic connections between neurons (i.e., changes in number and strength of synaptic connections); however, there were no methods for examining neurotransmitter release at individual synapses.

To address this problem, we have recently introduced a novel class of probes, termed Fluorescent False Neurotransmitters (FFNs) that act as fluorescent tracers of neurotransmitters (Figure 1).[9] Specifically, FFNs function as fluorescent substrates of transporter proteins that accumulate physiological neurotransmitters in synaptic vesicles (vesicular monoamine transporter 2 or VMAT2 for monoamine neurotransmitters such as dopamine), and thus enable visualization of individual synapses (accumulation of FFN) and their activity (release of FFN) in the brain tissue via two-photon microscopy.

Hydroarylation Guides the Design of Fluorescent False Neurotransmitters (FFNs)

The design of FFNs was influenced by the hydroarylation methodology developed in our laboratories. As FFNs are not fluorescent tags of biological macromolecules, but reporter substrates of monoamine transporter proteins, it is important to keep the size of the FFN condidates as small as possible, while maintaining high brightness and photostability. In this respect, coumarins are especially attractive and two design approaches were considered: 1) An endogenous neurotransmitter would be structurally modified to impart fluorescence to the product (e.g., conversion of serotonin to pyrrolocoumarin **5)**; and 2) A known coumarin fluorophore would be modified to incorporate the ethylamino group, the key recognition element for the relevant transporter proteins (e.g., modification of the laser dye **LD490**[10] to the agent **FFN511**, Figure 2).

In this context, we examined the scope of the intramolecular hydroarylation of aryl alkynoate esters catalyzed by $PtCl_4$ and $Au(PPh_3)SbF_6$, which revealed remarkably wide and complementary applicability of these methods for the synthesis of complex coumarins. These mild catalytic methods directly affect the design and development of FFN probes by providing the flexibility of placing diverse functional groups at the coumarin core, enabling the tuning of both the fluorescence properties and the ability to function as substrates for relevant protein targets (neurotransmitter transporters). This paper focuses on the substrate scope of the hydroarylations methods, while the pharmacological and biological studies will be described in the future in a separate publication.

Results and Discussion

Search for Competent Hydroarylation Catalysts. Screening of Platinum and Gold Complexes and Salts

According to the first design approach to potential FFN agents (Figure 1A), aryl alkynoate ester **8** was prepared and examined with the hydroarylation condition, using $PtCl_4$ as the catalyst developed in our laboratories (Table 1).[3,4] We were pleased to find that $PtCl_4$ (10 mol %) in a mixture of 1,4-dioxane:dichloroethane (DCE) [1:1] at 80 °C, effected the desired transformation in 8 hr, affording a 54% yield of the pyrrolocoumarin **9** (entry 1, Table 1). Formation of this strained compound as the only detectable product is noteworthy and the regioselectivity is discussed in detail below. Attempts to decrease the catalyst loading to 5 mol % led to a decrease in yield, however an increase in overall mass balance; after heating at 80 °C for 24 hr the product was isolated in 31% yield with 51% of the starting alkyne recovered (entry 2, Table 1).

For direct comparison, we examined the conditions developed by Fujiwara[11] (entry 3, Table 1), Echavarren[12] (entries 4 and 5, Table 1) and Fürstner[13] (entry 6, Table 1) for the activation of alkynes. Fujiwara's conditions, using $Pd(OAc)_2$ as the catalyst and TFA as a co-solvent, afforded neither the desired product **9** nor the substrate **8**, demonstrating the incompatibility of the acidic conditions with complex substrates. The loss of the Boc-protecting group in the presence of TFA exposes the primary aliphatic amine, which presumably deactivates to the palladium catalyst. The reactions employing $PtCl_2$ (5 mol %) were dependent on the solvent; toluene gave the highest yield (50%, entry 4). We viewed the higher mass balance of the $PtCl_4$ (5 mol %) reaction as well as our previous experience with this system as the key decision factors to explore the scope of the $PtCl_4$ system.

In addition to platinum catalysts, reports from Reetz,[14] Fürstner,[15] Echavarren,[16] Toste,[17] Shi[18] and others demonstrated high activity of gold complexes for hydroarylation and other procesess relying on alkyne activation.

Consequently, a variety of commonly employed gold salts were screened with and without silver salt additives. The most promising of the examined systems was the combination of $Au(PPh_3)Cl$ and $AgSbF_6$ (10 mol %) which furnished the product in 92% yield in only 5 min at room temperature (entry 1, Table 2). As a control we confirmed that the catalytic amount of $AgSbF_6$ (in the absence of gold) was inactive. Optimization of the catalyst loading for the $Au(PPh_3)Cl/AgSbF_6$ system revealed that the reaction proceeded equally well with 5 mol % (entry 2, Table 2). The product was also formed in high yield even in the presence of 1 mol % of the catalyst, however the reaction required heating to 80 °C for 6 hours. For the purpose of mapping the scope of the gold-silver system, we chose the mild room temperature conditions employing 5 mol % of the catalyst.

Finally, in order to rule out the possibility of Brønsted acid catalysis by either HCl or $HSbF_6$, formed *in situ* in DCE by the action of $PtCl_4$ or $AgSbF_6$ respectively,[19] we

conducted a screen of HCl, $HSbF_6$ and TfOH against substrates of various sensitivities to acid. None of the conditions explored succeeded in furnishing the hydroarylation products (see the supporting information). These results support the role of the transition metal Lewis acids as the active catalysts in the reaction.

The Regioselectivity of Catalytic Hydroarylation of Indole-Derived Substrates

As described above, the cyclization of substrate **8** proceeded with high regioselectivity, affording a single regioisomer, namely the sterically congested product **9** under both the Pt(IV) and Au(I) conditions (Scheme 2). The other regioisomer was not detected in the crude reaction mixture. It is worth noting that these products are forced into a helical conformation due to the major steric overlap of the alkyl substituents. In addition to the electronic rationale (see discussion below and Scheme 3), we also considered the possibility that the carbamate of the ethylamino group might serve as a directing group for the catalyst, favoring cyclization to the C-4 position.

To test this hypothesis substrate **10** was prepared and submitted to the cyclization conditions (Scheme 2). The $PtCl_4$ catalyzed reaction afforded product **11** in 54% yield, again as a single regioisomer annulated at C-4. This result demonstrates that the carbamate group is not responsible for the regioselectivity observed in the cyclization of substrates **8** and **15**. Interestingly, substrate **10** under the $Au(PPh_3)Cl/AgSbF_6$ conditions decomposed rapidly even at room temperature and analysis of the crude ^1H NMR failed to reveal any diagnostic signals for either regioisomer of the cyclized product. It is possible that the highly carbophilic gold cation underwent metallation of the indole nucleus at the C-3 position, followed by deleterious side reactions leading ultimately to the destruction of the substrate. In addition to putting the directing group hypothesis to rest, the substrates **8** and **10** revealed complementarity of the platinum and gold catalytic systems. The less active $PtCl_4$ catalyst can be advantageous in the case of more reactive substrates such as compound **10**.

Electronic Rationale for the Observed Regioselectivity

On this ground, we propose an electronic rationale for the regioselectivity observed with the indole substrates. Following coordination of the Lewis acid to the alkyne, the electrophilic attack can occur at either the C-4 or C-6 position of the benzene ring, affording intermediates **I** or **IV** respectively (Scheme 3). The intermediate **I** (and the corresponding transition state) can be stabilized via delocalization of the positive charge in the benzene ring (three resonance forms **I-III**) without disrupting the aromaticity of the pyrrole ring. In contrast, stabilization of intermediate **IV** requires delocalization of the positive charge in the pyrrole ring, thereby breaking its aromaticity (similar rationale explains the kinetic preference for aromatic electrophilic substitution of the more hindered 1-position of naphthalene). Thus, the first pathway has a lower energetic barrier, apparently by such an extent that the other regioisomer **13** is not observed. Although there is significant steric crowding between the substituents at C-3 and C-4, a close examination of the intermediate (**I-III**) reveals a "*gauche-like*" interaction due to the tetrahedral geometry at C-4. Upon deprotonation at C-4 and rehybridization of the carbon center as well as rearomatization, the product is formed and is locked in the strained conformation (following the protonative deplatination[3b]).

Cyclization of Highly Hindered Substrate 15

To test the limits of the hydroarylative cyclization and potentially force the formation of the other regioisomer, we prepared the sterically more demanding substrate **15** containing a phenyl ring attached to the alkyne (entry 4, Table 3). Remarkably, a single product was formed in 98% yield via the cyclization at the C-4 position under the gold catalyzed

conditions, while the platinum catalyst failed completely to provide any cyclized product. These results demonstrate the remarkable robusteness of the hydroarylative cyclization under the gold catalysis, lower reactivity of the platinum catalyst and the energetic inaccessibility of the C-6 cyclization pathway. The X-ray crystallographic structure of the product **14** was obtained and confirmed a significant degree of helicity to the aromatic core, with a dihedral angle of 19.4° (bond C_a-C_b, Figure 3). As can be seen in the ORTEP plot, the phenyl ring is held above the methylene group attached to the indole ring. The upfield shift of this methylene group seen in the ^{1}H NMR suggests significant shielding by the phenyl ring; 1.26 ppm versus 2.64 ppm in the substrate.

Substrate Scope of Indole-derived Substrates

The catalytic hydroarylation of indole substrates showed an excellent tolerance for both the functional groups and steric hindrance (Table 3). Both catalytic systems are compatible with the free indole amino group, Boc-protected aliphatic amine and Boc-protected α-amino ester groups. Furthermore, complementarity of the platinum and the gold-silver system was revealed; the former one being less active which becomes advantageous with more reactive substrates such as substrate **10**. Most notably, the cyclization showed exclusive regioselectivity for the 4-position, which we rationalize in terms of electronic factors, and is tolerant of considerable steric hindrance as demonstrated by the efficient formation of helical compound **14**.

Substrate Scope of Aryl Alkynoate Esters Containing Aniline Amino Groups

We next investigated the hydroarylative cyclization of aniline substrates. This was driven by the need to examine the importance of the aniline nitrogen substitution in the probe **FFN511** (Figure 1) on its interaction with monoamine transporters (e.g. VMAT2, see Introduction) and other CNS receptors.

The Boc-protected aniline substrate **18** underwent efficient cyclization with the $Au(PPh_3)Cl/AgSbF_6$ catalyst, providing a mixture of regioisomers **19** and **20** in 86% yield (entry 1, Table 4); whereas the same substrate failed to react in the presence of $PtCl_4$. Presumably, the relatively low electron donating ability of the carbamate substituent renders the arene ring unreactive towards the $PtCl_4$ activated alkyne. The free aniline **21** also failed to cyclize in the presence of $PtCl_4$, likely due to coordination of the catalyst to the free amine (entry 2, Table 4). In contrast, the gold system was well tolerant of free aniline giving a high yield of a mixture of coumarins **22** and **23** (95%). The success of the gold catalyst in this example is attributed to its high carbophilicity that leads to preferential coordination to the alkyne.

The tertiary anilines, on the other hand, are well tolerated under both catalytic conditions (compounds **24** and **27**, entries 3 and 4, Table 4). This is due to the stronger electron-donating ability of tertiary amines (as well as poorer metal-chelating ability). In addition, the carbazole derivative **29** performed well under both conditions (entry 5, Table 4). It is noteworthy that $PtCl_4$ catalyst afforded higher regioselectivity (1:5) in comparison to the $Au(PPh_3)Cl/AgSbF_6$ system (1:1.7). Thus, the less active catalyst is more selective for the more sterically congested product **30**, illustrating once again the importance of electronic factors in this transformation.

Synthesis of FFN511 and Candidates for a New Generation of FFN Probes

As discussed in the introduction the probe **FFN511** was the first example of fluorescent false neurotransmitters (FFNs) enabling for the first time visualization of neurotransmitter release from hundreds of individual presynaptic terminals in the brain.[9] **FFN511** is synthesized in short order from commercially available 8-hydroxyjulolidine (**32**) and the *N*-Boc-amino alkynoic acid **33** (Scheme 4). The ester coupling provides substrate **34**, which is

then cyclized in high yield under both sets of hydroarylation conditions; 91% and 95% employing Pt and Au systems, respectively (entry 1, Table 5). Simple deprotection with TFA furnished **FFN511** as a TFA salt (Scheme 4). This procedure has successfully been scaled up to 960 mg (2.5 mmol) providing suffient quantities of material for the biological studies.

Enouraging results with **FFN511**[9] prompted us to undertake a structure-activity relationship study of **FFN511** to identify the key recognition elements for the monoamine transporters while maintaining the coumarin core and the fluorescence properties. There are two major sites for modification of **FFN511**: 1) The aniline nitrogen in the 7-position and substitution in the adjacent positions (C-6 and C-8); and 2) the ethylamine side chain in the 4-position. The compatibility of the gold system with a range of anilines in the 7-position is described above (Table 4).

Modification of the *N*-Boc-protected ethylamino side chain was well tolerated, including α-methylamino substrate **36** and truncated methylamino substrate **38**, offering high yields of the desired products. The results of the hydroarylation of the *N*-allyl protected substrates (entries 4–6, Table 5) were particularly interesting as no hydroarylation of the alkene was observed under either reaction condition. For all of these substrates the alkyne was selectively activated, leading to the formation of the targets in high yield (90–93%) for the $Au(PPh_3)Cl/AgSbF_6$ conditions and moderate yields (74–76%) for the $PtCl_4$ system. The *N*-allyl group could be selectively deprotected with $Pd(PPh_3)_4$ (10 mol %) in THF in the presecence of *N,N′*-dimethylbarbituric acid, enabling futher modification of the secondary aniline amine.

The remarkably broad substrate scope of the hydroarylation methodology sets the stage for the preparation of a series of coumarin compounds, enabling the systematic examination of the substrate scope of monoamine transporters involved in accumulation of neurotransmitters in the presynaptic terminals. As a representative example, we show here the entire synthesis of a new FFN candidate, compound **PV139**, where the “upper ring” of the aniline substitution in **FFN511** was removed. The properly protected aminophenol **48** was synthesized from commercially available 5-hydroxyquinoline (**46**, Scheme 5) by hydrogenation under acidic conditions, phenol protection, *N*-allylation and phenol deprotection. This phenol was then condensed with the *N*-Boc-amino alkynoic acid **33**, to yield the aryl alkynoate substrate **44** and the hydroarylative cyclization furnished coumarin **45** (90% with the Au system). Deprotection of both amines delivered the compound **PV139** as a TFA salt in excellent yield. This approach allows for selective elaboration of either the aromatic amine or the primary aliphatic amine in either order, providing a versatile platform for the structure-activity study of these compounds in the context of FFN probe development.

Conclusions

In summary, we have examined two catalytic systems, which afford complex coumarins in good to excellent yields under mild conditions. While the $Au(PPh_3)Cl/AgSbF_6$ system demonstrated excellent compatibility with a variety of functional groups, $PtCl_4$ was found to be more sensitive to the electronic factors of the arene substrates. Both catalysts, however, performed well in the presence of a variety of functional groups including Boc-protected amines, tertiary anilines, allylic anilines, protected α-aminoesters, and free (NH)-indoles and carbazoles. Although the platinum system is less active, it revealed higher regioselectivity in some instances and out-performed the gold catalyst with indole substrates lacking substitution at the C-3 position.

The synthetic methods examined herein enable an SAR study of the FFN probes, where **FFN511** serves as the lead compound, with the aim to develop second generation FFN probes with improved functional parameters for imaging synaptic activity in the brain. Indeed, the chemistry is in place for examining the importance of the aniline amine substitution in the 7-positions (and the adjacent positions on the arene ring) as well as the substitution and the linker of the primary amine. The results of these biological and pharmacological studies will be reported in the future. In general, the mild catalytic methods complement the von Pechman condensation and other classical methods for coumarin synthesis.

Experimental Section

General Considerations

Argon was purified by passage through Drierite. Nuclear Magnetic Resonance spectra were recorded at 300 K. ^{1}H NMR spectra recorded in $CDCl_3$ solutions were referenced to TMS (0.00 ppm). ^{13}C NMR spectra recorded in $CDCl_3$ were referenced to the residual solvent peak (77.16 ppm). ^{19}F NMR spectra were recorded in CD_3OD with α,α,α-trifluorotoluene (10 μL) as an internal standard. The spectra were referenced to the α,α,α-trifluorotoluene fluorine peak, −63.72 ppm. Several compounds containing the carbamate group were found to exist in rotameric forms. As such, NMR spectra were recorded at elevated temperatures in order to produce clearer spectra. Flash chromatography was performed on silica gel (230–400 mesh). High-resolution mass spectra (HRMS) were acquired on a high resolution sector type double focusing mass spectrometer (ionization mode: FAB+). Reactions were monitored by TLC analysis using hexanes/ethyl acetate mixtures as the eluent and visualized using permanganate stain and/or cerric ammonium molybdate stain and/or UV light. Toluene, acetonitrile, tetrahydrofuran, ethyl ether, and dichloromethane were dried via passage through a column of activated alumina. Chloroform-*d*$_1$ was stored over 4Å molecular sieves. $PtCl_4$ (99.9%-Pt), $Au(PPh_3)Cl$ (99.9+%-Au), and $AgSbF_6$ (98%) were purchased from Strem Chemicals Inc. and used as received. 1,2-Dichloroethane (DCE) and 1,4-dioxane were used as received without any further purification.

General Procedure for the Synthesis of Aryl Alkynoates via DIC coupling of Phenols and Propiolic Acids

To a flame dried round bottom flask equipped with a magnetic stir bar was added the appropriate alkynoic acid (1.2 eq.) followed by dry DCM (0.3 M). The solution was sealed under argon with a rubber septum and cooled to 0 °C in an ice/brine bath. Neat *N*,*N*′-diisopropylcarbodiimide (DIC) (1.5 eq.) was added via syringe and stirred for 1 minute during which a white precipitate formed. The appropriate phenol (1 eq.) was dissolved in dry DCM (1 M) and added via syringe. Lastly, 4-dimethylaminopyridine (DMAP) (25 mol %) was dissolved in dry DCM (0.5 M) and added dropwise to the stirring solution. The mixture was stirred under argon at 0 °C until the phenol was consumed as determined by TLC. The reaction was then filtered through celite and concentrated *in vacuo*. The residue was then purified via flash column chromatography.

Representative DIC Coupling Procedure for the Formation of Substrate 3-(2-(*tert*-butoxycarbonylamino)ethyl)-1*H*-indol-5-yl but-2-ynoate (8)—To a flame dried round bottom flask equipped with a stir bar was added 2-butynoic acid (202 mg, 2.4 mmol) followed by dry DCM (8 mL). The solution was sealed under argon with a rubber septum and cooled to 0 °C in an ice/brine bath. Neat DIC (470 μL, 3.0 mmol) was added via syringe and stirred for 1 minute during which a white precipitate formed. A solution of *N*-Boc-serotonin[20] (552 mg, 2.0 mmol) in dry DCM (1 mL) was added to the reaction mixture via syringe. Lastly, DMAP (61 mg, 0.5 mmol) was dissolved in dry DCM (1 mL) and added

dropwise to the stirring solution. The reaction was stirred under argon at 0 °C until complete consumption of the phenol was observed by TLC (2 hr). The reaction was then filtered through celite and concentrated *in vacuo*. The residue was then purified via column chromatography, 20% EtOAc/Hexanes, to afford **3-(2-(*tert*-butoxycarbonylamino)ethyl)-1*H*-indol-5-yl but-2-ynoate** (**8**) as an amorphous white solid (670 mg, 98%). **^{1}H NMR ($CDCl_3$, 300 MHz)** δ 1.44 (s, 9H); 2.04 (s, 3H); 2.83 (t, *J* = 6.6 Hz, 2H); 3.36 (br q, *J* = 6.0 Hz, 2H); 4.71 (br s, 1H); 6.90-6.86 (m, 2H); 7.28-7.21 (m, 2H); 8.75 (br s, 1H); **^{13}C NMR ($CDCl_3$, 75 MHz)** δ 4.0, 25.6, 28.5, 41.0, 72.5, 79.3, 87.9, 110.7, 111.9, 113.3, 115.8, 123.9, 127.7, 134.6, 143.5, 153.3, 156.2. **HRMS (FAB+):** calculated for $C_{19}H_{22}N_2O_4$ 342.1580, measured 342.1580 [M].

1*H*-indol-5-yl but-2-ynoate (10) was eluted with 10% EtOAc:Hex as an amorphous white solid (480 mg, 70%). **^{1}H NMR ($CDCl_3$, 400 MHz)** δ 2.04 (s, 3H); 6.50 (dd, *J* = 2.8 Hz, 0.8 Hz, 1H); 6.93 (dd, *J* = 8.4 Hz, *J* = 2.0 Hz, 1H); 7.16 (t, 2.8 Hz, 1H); 7.26 (d, *J* = 8.4 Hz, 1H); 7.36 (d, *J* = 2.4 Hz, 1H); 8.25 (s, 1H); **^{13}C NMR ($CDCl_3$, 100 MHz)** δ 4.1, 72.5, 88.0, 103.0, 111.7, 112.7, 115.7, 125.9, 128.1, 134.0, 143.8, 153.3. **HRMS (FAB+):** calculated for $C_{12}H_9NO_2$ 199.0633, measured 199.0641 [M].

3-(2-(*tert*-butoxycarbonylamino)ethyl)-1*H*-indol-5-yl 3-phenylprop-2-ynoate (15) was eluted with 20% EtOAc:Hex as an amorphous white solid (736 mg, 91%). **^{1}H NMR ($CDCl_3$, 300 MHz)** δ 1.45 (s, 9H); 2.90 (t, *J* = 6.9 Hz, 2H); 3.42 (b quart, *J* = 6.3 Hz, 2H); 4.63 (bs, 1H); 7.00 (dd, *J* = 2.1 Hz, *J* = 8.7 Hz, 2H); 7.48-7.32 (m, 5H); 7.63 (d, *J* = 8.4 Hz, 2H); 8.37 (bs, 1H); **^{13}C NMR ($CDCl_3$, 100 MHz)** δ 25.8, 28.5, 41.0, 79.4, 80.7, 88.5, 110.9, 112.0, 113.4, 115.8, 119.5, 123.9, 127.8, 128.8, 131.0, 133.2, 134.6, 143.5, 153.7, 156.2. **HRMS (FAB+):** calculated for $C_{24}H_{24}N_2O_4$ 404.1736, measured 404.1730 [M].

3-(2-(*tert*-butoxycarbonylamino)-3-methoxy-3-oxopropyl)-1*H*-indol-5-yl but-2-ynoate (16) was prepared from *N*-Boc-5-hydroxytryptophan methyl ester[21] eluted with 6% EtOAc:DCM as an amorphous white solid (430 mg, 95%). **^{1}H NMR ($CDCl_3$, 400 MHz)** δ 1.35 + 1.44 (s,s, 9H, rotomers); 2.06 (s, 3H); 3.20 (bd, *J* = 4.0 Hz, 2H); 3.65 (s, 3H); 4.59 (br q, *J* = 7.2, 1H); 5.14 (d, *J* = 7.6 Hz, 1H); 6.92-6.86 (m, 2H); 7.23-7.19 (m, 2H); 8.72 (s, 1H); **^{13}C NMR ($CDCl_3$, 100 MHz)** δ 4.0, 27.9, 28.3, 52.4, 54.2, 72.3, 80.1, 88.0, 110.1, 110.6, 112.0, 115.8, 124.7, 127.9, 134.3, 143.6, 153.3, 155.3, 172.7. **HRMS (FAB+):** calculated for $C_{21}H_{24}N_2O_6$ 400.1634, measured 400.1637 [M].

3-(*tert*-butoxycarbonylamino)phenyl but-2-ynoate (18) was eluted with 10% EtOAc:Hex as an amorphous white solid (1.03 g, 74%). **^{1}H NMR ($CDCl_3$, 400 MHz)** δ 1.50 (s, 9H); 2.04 (s, 3H); 6.78 (d, *J* = 8.8 Hz, 2H); 7.10 (d, *J* = 8.4 Hz, 1H); 7.25 (t, *J* = 8.0 Hz, 1H); 7.25 (s, 1H); **^{13}C NMR ($CDCl_3$, 100 MHz)** δ 4.0, 28.3, 72.0, 80.8, 88.3, 111.7, 115.7, 116.1, 129.7, 139.8, 150.5, 152.0, 152.5. **HRMS (FAB+):** calculated for $C_{15}H_{17}NO_4$ 275.1158, measured 275.1168 [M].

3-aminophenyl but-2-ynoate (21)—To a solution of **3-(*tert*-butoxycarbonylamino)phenyl but-2-ynoate (18)** (812 mg, 2.9 mmol) in DCM (15 mL) at 0 °C was added trifluoroacetic acid (TFA) (5 mL) dropwise. The mixture was stirred at 0 °C for 1 hr. The solvent was then removed *in vacuo* and the resulting residue was dissolved in DCM (10 mL) and slowly quenched with $NaHCO_3$ (aq. satd.). The organic layer was separated and dried over $MgSO_4$. The suspension was filtered and the filtrate was concentrated. The residue was chromatographed on silica gel, eluting with 20% EtOAc:Hex, to yield **3-aminophenyl but-2-ynoate (21)** (505 mg, 98%) as an amorphous white solid. **^{1}H NMR ($CDCl_3$, 400 MHz)** δ 2.01 (s, 3H); 3.77 (br s, 2H); 6.38 (dd, *J* = 5.2 Hz, 2.0 Hz, 1H); 6.51-6.45 (m, 2H); 7.10 (dt, *J* = 8.0 Hz, *J* = 1.2 Hz, 1H); **^{13}C NMR ($CDCl_3$, 100 MHz)** δ

13.8, 72.1, 88.1, 107.8, 110.8, 113.0, 130.0, 148.0, 150.9, 152.0. **HRMS (FAB+):** calculated for $C_{10}H_{10}NO_2$ 176.0712, measured 176.0704 [M+1].

***tert*-butyl-4-(3-(but-2-ynoyloxy)phenyl)piperazine-1-carboxylate (24)** was eluted with 10% EtOAc:Hex as an amorphous white solid (951 mg, 92%). **^{1}H NMR ($CDCl_3$, 400 MHz)** δ 1.48 (s, 9H); 2.05 (s, 3H); 3.13 (br t, *J* = 6.0 Hz, 4H); 3.56 (t, *J* = 5.6 Hz, 4H); 6.62 (m, 1H, eclipsed by proton at 6.64 ppm); 6.64 (s, 1H); 6.79 (d, *J* = 9.2 Hz, 1H); 7.25 (t, *J* = 8.0 Hz, 1H); **^{13}C NMR ($CDCl_3$, 100 MHz)** δ 4.0, 28.5, 48.9, 72.2, 80.0, 88.0, 109.2, 112.6, 114.1, 129.9, 151.0, 152.0, 152.4, 154.7. **HRMS (FAB+):** calculated for $C_{19}H_{24}N_2O_4$ 344.1736, measured 344.1746 [M].

8-(2,3,6,7-tetrahydro-1H,5H-benzo[ij]quinolizine)-but-2-ynoate (27) was eluted with 5% EtOAc:Hex as an amorphous beige solid (809, 79%). **^{1}H NMR ($CDCl_3$, 300 MHz)** δ 1.99-1.89 (m, 4H); 2.04 (s, 3H); 2.58 (t, *J* = 6.3 Hz, 2H); 2.72 (t, *J* = 6.3 Hz, 2H); 3.14-3.09 (m, 4H); 6.25 (d, *J* = 8.1 Hz, 1H); 6.76 (d, *J* = 8.1 Hz, 1H); **^{13}C NMR ($CDCl_3$, 100 MHz)** δ 4.0, 21.2, 21.6, 21.9, 27.6, 49.4, 49.9, 72.3, 87.4, 108.4, 113.4, 119.6, 127.0, 144.0, 146.7, 152.3. **HRMS (FAB+):** calculated for $C_{16}H_{17}NO_2$ 255.1259, measured 255.1257 [M].

9*H*-carbazol-2-yl but-2-ynoate (29) was eluted with 10% EtOAc:Hex as an amorphous white solid (302 mg, 40%). **^{1}H NMR ($CDCl_3$, 400 MHz)** δ 2.07 (s, 3H); 6.96 (dd, *J* = 8.4 Hz, *J* = 2.0 Hz, 1H); 7.15 (s, 1H); 7.25-7.21 (m, 1H); 7.40-7.33 (m, 2H); 7.96 (t, *J* = 6.8 Hz, 2H); 8.11 (s, 1H); **^{13}C NMR ($CDCl_3$, 100 MHz)** δ 4.2, 72.3, 88.5, 103.8, 110.8, 113.0, 119.8, 120.3, 121.0, 121.7, 122.8, 125.9, 139.7, 140.2, 148.4, 152.8. **HRMS (FAB+):** calculated for $C_{16}H_{11}NO_2$ 249.0790, measured 249.0801 [M].

5-(*tert*-butoxycarbonylamino)pent-2-ynoic acid (33)—To a solution of ***tert*-butyl but-3-ynyl(tosyl)carbamate**[22] (3.23 g, 10 mmol) in methanol (100 mL) was added Mg turnings (2.43 g, 100 mmol). The resulting mixture was sonicated for 2 hr at which time all of the Mg had dissolved. The reaction volume was reduced to ~20 mL *in vacuo*. The solution was then diluted with DCM (50 mL) and poured into aq. HCl (0.5 M, 50 mL). The resulting magnesium salts were filtered. The organic phase was separated and the aqueous solution was extracted with EtOAc. The organic layers were combined and washed with satd. $NaHCO_3$ (aq). The organic layer was dried over $MgSO_4$ and concentrated *in vacuo*. The resulting residue was purified via flash column (50% DCM/Hex) to afford ***tert*-butyl but-3-ynylcarbamate** (1.54 g, 9.1 mmol) as a colorless oil, 91%. **^{1}H NMR ($CDCl_3$, 400 MHz)** δ 1.35 (s, 9H); 1.92 (t, *J* = 2.0 Hz, 1H); 2.29-2.26 (m, 2H); 3.18-3.17 (m, 2H); 5.01 (br s, 1H); **^{13}C NMR ($CDCl_3$, 100 MHz)** δ 19.9, 28.3, 39.3, 69.8, 79.3, 81.6, 155.8. This material (4.4 g, 26.0 mmol) in THF (150 mL) was cooled to −30 °C under argon. To the resulting solution was added MeLi (1.4 M in pentane, 40.9 mL, 57 mmol) dropwise. The cloudy solution was stirred for 30 mins. The flask was then equipped with a vent needle and a CO_2 bubbler, such that the gas bubbled through the reaction solution. After 2 hrs the reaction was quenched with H_2O (~100 mL) and neutralized with HCl (1 M). The solution was then extracted with EtOAc and the organic layer was dried over $MgSO_4$. The solvent was removed *in vacuo* to afford a thick pale yellow oil which was placed under vacuum. While under vacuum the oil solidified. The solid was then triturated with hexanes to yield **5-(*tert*-butoxycarbonylamino)pent-2-ynoic acid (33)** (5.05 g, 23.6 mmol) as an amorphous white solid, 91%. **^{1}H NMR ($CDCl_3$, 400 MHz, 350 K)** δ 1.46 (s, 9H); 2.54 (t, *J* = 6.4 Hz, 2H); 3.32 (s, 2H); 5.23 (br s, 1H); 9.64 (br s, 1H); **^{13}C NMR ($CDCl_3$, 75 MHz, 350 K)** δ 20.6, 28.6, 39.3, 74.6, 81.0, 88.0, 155.8, 156.7. **HRMS (FAB+):** calculated for $C_{10}H_{16}NO_4$ 214.1079, measured 214.1070 [M+1].

8-(2,3,6,7-tetrahydro-1H,5H-benzo[ij]quinolizine)-(5-(*tert*-butoxycarbonylamino)pent-2-ynoate) (34) was eluted with 5% EtOAc/DCM as an

amorphous white solid (580 mg, 98%). **^{1}H NMR ($CDCl_3$, 300 MHz)** δ 1.46 (s, 9H); 1.97-1.92 (m, 4H); 2.58 (t, *J* = 6.6 Hz, 4H); 2.72 (t, *J* = 6.3 Hz, 2H); 3.14-3.09 (m, 4H); 3.33 (apparent quartet, *J* = 6.3 Hz, 2H); 4.91 (br s, 1H); 6.25 (d, *J* = 7.8 Hz, 1H); 6.76 (d, *J* = 8.1 Hz, 1H); **^{13}C NMR ($CDCl_3$, 75 MHz)** δ 20.6, 21.2, 21.6, 21.9, 27.5, 28.4, 38.6, 49.4, 49.9, 73.8, 79.8, 88.7, 108.4, 113.4, 119.7, 127.0, 144.0, 146.7, 152.1, 155.7. **HRMS (FAB+):** calculated for $C_{22}H_{28}N_2O_4$ 384.2049, measured 384.2046 [M].

8-(2,3,6,7-tetrahydro-1H,5H-benzo[ij]quinolizine)-(5-(*tert*-butoxycarbonylamino)hex-2-ynoate) (36) was eluted with 10% EtOAc/Hex as an amorphous white solid (290 mg, 55%). **^{1}H NMR ($CDCl_3$, 300 MHz)** δ 1.22 (d, *J* = 6.6 Hz, 3H); 1.45 (s, 9H); 1.96-1.91 (br m, 4H); 2.60-2.56 (m, 4H); 2.72 (t, *J* = 6.6 Hz, 2H); 3.14-3.09 (m, 4H); 3.91 (br s, 1H); 4.67 (br s, 1H); 6.26 (d, *J* = 8.1 Hz, 1H); 6.77 (d, *J* = 8.4 Hz, 1H); **^{13}C NMR ($CDCl_3$, 75 MHz)** δ 19.8, 21.1, 21.5, 21.8, 26.6, 27.5, 28.4, 44.4, 49.4, 49.8, 74.7, 79.6, 87.9, 108.4, 113.3, 119.6, 126.9, 144.0, 146.8, 152.0, 154.9. **HRMS (FAB+):** calculated for $C_{23}H_{30}N_2O_4$ 398.2206, measured 398.2198 [M].

8-(2,3,6,7-tetrahydro-1H,5H-benzo[ij]quinolizine)-(4-(*tert*-butoxycarbonylamino)but-2-ynoate) (38) was eluted with 10% EtOAc/Hex as an amorphous white solid (330 mg, 40%). **^{1}H NMR ($CDCl_3$, 400 MHz)** δ 1.47 (s, 9H); 1.94 (sext, *J* = 6.4 Hz, 4H); 2.56 (t, *J* = 6.8 Hz, 2H); 2.72 (t, *J* = 6.8 Hz, 2H); 3.12 (quart, *J* = 5.6 Hz, 4H); 4.14 (br d, *J* = 4.8 Hz, 2H); 4.86 (br s, 1H); 6.25 (d, *J* = 8.0 Hz, 1H); 6.77 (d, *J* = 8.0 Hz, 1H); **^{13}C NMR ($CDCl_3$, 100 MHz)** δ 21.2, 21.6, 21.9, 27.6, 28.4, 30.6, 49.4, 49.9, 74.8, 80.7, 85.8, 108.3, 113.3, 119.8, 127.1, 144.1, 146.5, 151.8, 155.2. **HRMS (FAB+):** calculated for $C_{21}H_{26}N_2O_4$ 370.1893, measured 370.1882 [M].

1-allyl-1,2,3,4-tetrahydroquinolin-7-yl 5-(*tert*-butoxycarbonylamino)pent-2-ynoate (40) was eluted with 15% EtOAc/Hex as a yellow oil (970 mg, 91%). **^{1}H NMR ($CDCl_3$, 300 MHz)** δ 1.46 (s, 9H); 1.94 (quint, *J* = 6.3 Hz, 2H); 2.59 (t, *J* = 6.3 Hz, 2H); 2.73 (t, *J* = 6.3 Hz, 2H); 3.27 (t, *J* = 5.7 Hz, 2H); 3.34 (quart, *J* = 6.3 Hz, 2H); 3.82 (dd, *J* = 3.3 Hz, *J* = 1.5 Hz, 2H); 4.87 (br s, 1H) 5.20-5.13 (m, 2H); 5.87-5.74 (m, 1H); 6.24 (d, *J* = 2.1 Hz, 1H); 6.30 (dd, *J* = 8.0 Hz, *J* = 2.1 Hz, 1H); 6.91 (d, *J* = 8.1 Hz, 1H); **^{13}C NMR ($CDCl_3$, 75 MHz)** δ 20.4, 22.0, 27.6, 28.3, 38.5, 48.8, 53.6, 73.9, 79.6, 88.7, 103.5, 107.8, 116.1, 120.3, 129.3, 132.6, 146.1, 149.4, 152.1, 155.7. **HRMS (FAB+):** calculated for $C_{22}H_{28}N_2O_4$ 384.2049, measured 384.2041 [M].

1-allyl-1,2,3,4-tetrahydroquinolin-7-yl 5-(*tert*-butoxycarbonylamino)hex-2-ynoate (42) was eluted with 10% EtOAc/Hex as an amorphous pale yellow solid (759 mg, 95%). **^{1}H NMR ($CDCl_3$, 400 MHz)** δ 1.22 (d, *J* = 6.8 Hz, 3H); 1.44 (s, 9H); 1.92 (qunit, *J* = 5.6 Hz, 2H); 2.62-2.51 (m, 2H); 2.71 (t, *J* = 6.4 Hz, 2H); 3.25 (t, *J* = 5.6 Hz, 2H); 3.80 (d, *J* = 4.8 Hz, 2H); 3.90 (br s, 1H) 4.74 (br d, *J* = 7.6 Hz, 1H); 5.18-5.12 (m, 2H); 5.83-5.74 (m, 1H); 6.22 (d, *J* = 2.0 Hz, 1H); 6.28 (dd, *J* = 8.0 Hz, *J* = 2.0 Hz, 1H); 6.89 (d, *J* = 8.0 Hz, 1H); **^{13}C NMR ($CDCl_3$, 100 MHz)** δ 19.7, 22.0, 26.5, 27.6, 28.3, 44.3, 48.8, 53.6, 74.8, 79.5, 87.9, 103.5, 107.8, 116.1, 120.3, 129.3, 132.6, 146.1, 149.5, 152.1, 154.9. **HRMS (FAB+):** calculated for $C_{23}H_{30}N_2O_4$ 398.2206, measured 398.2218 [M].

1-allyl-1,2,3,4-tetrahydroquinolin-5-yl 5-(*tert*-butoxycarbonylamino)pent-2-ynoate (44) was eluted with 15% EtOAc/Hex as an amorphous pale yellow solid (95 mg, 64%). **^{1}H NMR ($CDCl_3$, 400 MHz)** δ 1.46 (s, 9H); 1.93 (t, *J* = 6.0 Hz, 2H); 2.62-2.59 (m, 4H); 3.26 (t, *J* = 6.0 Hz, 2H); 3.34 (quart, *J* = 6.0 Hz, 2H); 3.88-3.86 (m, 2H); 4.91 (s, 1H); 5.21-5.13 (m, 2H); 5.87-5.78 (m, 1H); 6.33 (dd, *J* = 8.0 Hz, *J* = 0.8 Hz, 1H); 6.45 (d, *J* = 8.0 Hz, 1H); 7.02 (t, *J* = 8.0 Hz, 1H); **^{13}C NMR ($CDCl_3$, 100 MHz)** δ 20.6, 21.4, 21.7, 28.5, 38.6, 48.7, 54.3, 73.8, 79.9, 88.8, 108.7, 109.3, 114.4, 116.2, 127.2, 133.1, 146.7, 148.4, 151.9, 155.7. **HRMS (FAB+):** calculated for $C_{22}H_{24}N_2O_4$ 384.2049, measured 384.2044 [M].

General Procedure for the Hydroarylation of Aryl-Alkynoates

All reactions were conducted at 0.05 M (concentration of substrate) in 1:1 mixture of DCE to 1,4-dioxane with 5 mol % catalyst. The solid catalyst was weighed into an 8 mL glass vial equipped with a magnetic stir bar. A stock solution of 1:1 DCE and 1,4-dioxane was then added to the vial, followed by a solution of the substrate in 1:1 DCE and 1,4-dioxane. The vial was then sealed under air with a solid Teflon lined screw-cap and heated to the appropriate temperature. The reactions were monitored by TLC. Upon consumption of the starting material, the solvent was removed *in vacuo* and the residue was chromatographed to afford pure product.

Representative Procedure for the $PtCl_4$ Catalyzed Cyclization of Substrate 3-(2-(*tert*-butoxycarbonylamino)ethyl)-1*H*-indol-5-yl but-2-ynoate (8)—To an 8 mL glass vial was added $PtCl_4$ (7.0 mg, 0.02 mmol) followed by a magnetic stir bar. A stock solution of 1:1 DCE and 1,4-dioxane (5 mL) was then added to the vial, followed by a solution of **3-(2-(*tert*-butoxycarbonylamino)ethyl)-1*H*-indol-5-yl but-2-ynoate (8)** (137 mg, 0.4 mmol) in 3 mL 1:1 DCE and 1,4-dioxane. The vial was then sealed under air with a Teflon screw cap and heated to 80 °C. The reaction was monitored by TLC. Upon complete consumption of the starting material the solvent was removed *in vacuo* and the residue was chromatographed, eluting with 10% EtOAc/DCM, to afford ***tert*-butyl-9-methyl-pyrano[3,2-*e*]indol-7(*3H*)-one-1-ethylcarbamate (9)** (74 mg, 54%) as an amorphous yellow solid. **^{1}H NMR (MeOD-d_4, 400 MHz)** δ 1.40 (s, 9H); 2.73 (s, 3H); 3.15 (t, J = 7.6 Hz, 2H); 3.27 (br q, J = 6.0 Hz, 1H); 6.25 (s, 1H); 6.66 (s, 1H); 7.08 (d, J = 8.8 Hz, 1H); 7.35 (s, 1H); 7.61 (d, J = 8.8 Hz, 1H); **^{13}C NMR (DMSO-d_6, 100 MHz)** δ 24.4, 28.2, 30.4, 41.0, 77.5, 110.8, 112.9, 113.0, 113.2, 116.9, 120.8, 127.4, 134.4, 150.3, 154.1, 155.5, 160.0. **HRMS (FAB+):** calculated for $C_{19}H_{22}N_2O_4$ 342.1580, measured 342.1582 [M]. The presence of the 2 doublets (7.08 and 7.61 ppm), but no triplet in the aromatic region of the ^{1}H NMR spectrum indicates cyclization to the C-4 position.

Representative Procedure for the $Au(PPh_3)Cl/AgSbF_6$ Catalyzed Cyclization of Substrate 3-(2-(*tert*-butoxycarbonylamino)ethyl)-1*H*-indol-5-yl but-2-ynoate (8) —To an 8 mL glass vial was added $Au(PPh_3)Cl$ (10 mg, 0.02 mmol) and $AgSbF_6$ (7 mg, 0.02 mmol) followed by a magnetic stir bar. A stock solution of 1:1 DCE and 1,4-dioxane (5 mL) was then added to the vial, followed by a solution of **3-(2-(*tert*-butoxycarbonylamino)ethyl)-1*H*-indol-5-yl but-2-ynoate (8)** (137 mg, 0.4 mmol) in 3 mL 1:1 DCE and 1,4-dioxane. The vial was then sealed under air with a Teflon screw cap and stirred at room temperature. The reaction was monitored by TLC. Upon complete consumption of the starting material the solvent was removed *in vacuo* and the residue was chromatographed, eluting with 10% EtOAc/DCM, to afford ***tert*-butyl-9-methyl-pyrano[3,2-*e*]indol-7(*3H*)-one-1-ethylcarbamate (9)** (129 mg, 93%) as an amorphous yellow solid.

9-methyl-pyrano[3,2-*e*]indol-7(*3H*)-one (11) was eluted with 30% EtOAc:Hex as an amorphous white solid (22 mg, 54% with [Pt]) **^{1}H NMR (DMSO-d_6, 400 MHz)** δ 2.70 (s, 3H); 6.32 (s, 1H); 6.88 (d, J = 2.4 Hz, 1H); 7.15 (d, J = 8.8 Hz, 1H); 7.60 (d, J = 2.8 Hz, 1H); 7.69 (d, J = 8.8 Hz, 1H); 11.70 (s, 1H). **HRMS (FAB+):** calculated for $C_{12}H_9NO_2$ 199.0633, measured 199.0643 [M].

***tert*-butyl-9-phenyl-pyrano[3,2-*e*]indol-7(*3H*)-one-1-ethylcarbamate (14)** was eluted with 40% EtOAc:Hex as an amorphous yellow solid (79 mg, 98% with [Au]). The resulting solid was dissolved in hot EtOAc, followed by the dropwise addition of hexanes until the solution became slightly turbid. The solution was then allowed to cool undisturbed. This procedure afforded yellow crystals sufficient for X-ray crystallographic analysis. **^{1}H NMR (DMSO-**

***d*$_6$, 400 MHz)** δ 1.26 (t, *J* = 7.2 Hz, 2H); 1.32 (s, 9H); 2.64 (quart, *J* = 6.4 Hz, 2H); 6.28-6.25 (m, 1H, eclipsed by a proton at 6.28 ppm); 6.28 (s, 1H); 7.18 (d, *J* = 2.0 Hz, 1H); 7.20 (d, *J* = 8.8 Hz, 1H); 7.48-7.37 (m, 5H); 7.70 (d, *J* = 8.8 Hz, 1H); 11.45 (s, 1H); **^{13}C NMR (DMSO-*d*$_6$, 75 MHz)** δ 26.9, 28.2, 77.2, 110.3, 110.8, 113.4, 114.4, 117.3, 121.4, 127.0, 127.8, 128.7, 129.3, 134.6, 139.6, 150.7, 155.2, 155.9, 160.2 (one carbon eclipsed by the residual solvent peak). **HRMS (FAB+):** calculated for $C_{24}H_{24}N_2O_4$ 404.1736, measured 404.1729 [M]. **Melting point:** 216.7-218.3 °C. X-ray structure was also obtained, see supporting information.

1-(2-(*tert*-butoxycarbonylamino)-methyl-propanoate)-9-methyl-pyrano[3,2-*e*]indol-7(3*H*)-one (17) was eluted with 15% EtOAc:DCM as an amorphous pale yellow solid (27 mg, 50% with [Pt]; 128 mg, 80% with [Au]). **^{1}H NMR (CDCl$_3$, 400 MHz, 350 K)** δ 1.34 (s, 9H); 2.73 (s, 3H); 3.35-3.33 (m, 1H); 3.55-3.52 (m, 1H); 3.59 (s, 3H); 4.52 (s, 1H); 6.27 (s, 1H); 7.17 (d, *J* = 8.4, 1H); 7.25 (s, 1H); 7.51 (d, *J* = 8.4 Hz, 1H); **^{13}C NMR (CDCl$_3$, 75 MHz, 350 K)** δ 25.1, 28.4, 33.6, 52.2, 55.0, 80.4, 112.1, 113.0, 114.5, 114.6, 116.3, 122.0, 127.2, 135.0, 151.8, 153.2, 155.2, 161.1, 172.6. **HRMS (FAB+):** calculated for $C_{21}H_{24}N_2O_6$ 400.1634, measured 400.1622 [M].

***tert*-butyl 4-methyl-2-oxo-2*H*-chromen-7-ylcarbamate (19)** was eluted with 15% EtOAc:Hex as an amorphous yellow solid (isolated as a 3.5:1 mixture of **19:20**; 95 mg, 86% with [Au]). **^{1}H NMR (CDCl$_3$, 500 MHz)** δ 1.51 (s, 9H); 2.37 (s, 3H); 6.14 (s, 1H); 7.14 (s, 1H); 7.37 (d, *J* = 10 Hz, 1H); 7.43 (s, 1H); 7.47 (d, *J* = 10 Hz, 1H); **^{13}C NMR (CDCl$_3$, 125 MHz)** δ 18.7, 28.4, 81.5, 105.7, 112.8, 114.5, 115.1, 125.3, 142.3, 152.4, 152.6, 154.5, 161.5. **HRMS (FAB+):** calculated for $C_{15}H_{17}NO_4$ 275.1158, measured 275.1160 [M].

***tert*-butyl 4-methyl-2-oxo-2*H*-chromen-5-ylcarbamate (20)** was eluted with 15% EtOAc:Hex as an amorphous yellow solid (isolated as a 3.5:1 mixture of **19:20**; 95 mg, 86% with [Au]). **^{1}H NMR (CDCl$_3$, 500 MHz)** δ 1.51 (s, 9H); 2.61 (s, 3H); 6.24 (s, 1H); 6.43 (s, 1H); 7.23 (d, *J* = 10 Hz, 1H); 7.32 (d, *J* = 5 Hz, 1H); 7.46 (t, *J* = 10 Hz, 1H). **HRMS (FAB+):** calculated for $C_{15}H_{17}NO_4$ 275.1158, measured 275.1160 [M].

7-amino-4-methyl-2*H*-chromen-2-one (22) co-eluted with **23**, however pure fractions of **22** were obtained via column chromatography eluting with 40% EtOAc:Hex to afford the product as an amorphous yellow solid (isolated as a 1:1 mixture of **22:23**; 100 mg, 95% with [Au]). **^{1}H NMR (MeOD-*d*$_3$:CDCl$_3$, 500 MHz, calibrated to residual MeOH peak, 3.33 ppm)** δ 2.36 (s, 3H); 5.96 (s, 1H); 6.53 (s, 1H); 6.62 (d, *J* = 10 Hz, 1H); 7.38 (d, *J* = 10 Hz, 1H). **^{13}C NMR (MeOD-*d*$_3$:CDCl$_3$, 500 MHz, calibrated to residual MeOH peak, 49.00 ppm)** δ 18.1, 100.0, 108.4, 110.6, 111.9, 125.7, 151.8, 154.4, 155.3, 163.2. **HRMS (FAB+):** calculated for $C_{10}H_{10}NO_2$ 176.0712, measured 176.0710 [M+1].

5-amino-4-methyl-2*H*-chromen-2-one (23) eluted as an inseparable mixture with **22** eluting with 40% EtOAc:Hex, affording the product as an amorphous yellow solid (isolated as a 1:1 mixture of **22:23**; 100 mg, 95% with [Au]). Given the isolation of pure **22**, analysis of the spectrum containing both **22** and **23** allowed for the identification of the peaks corresponding solely to product **23**. The shifts of the peaks identified in this manner, those related to **23**, are reported here. **^{1}H NMR (MeOD-*d*$_3$:CDCl$_3$, 500 MHz, calibrated to residual MeOH peak, 3.33 ppm)** δ 2.68 (s, 3H); 6.02 (s, 1H); 6.65-6.60 (m, 2H, overlaps with **22** doublet 6.62); 7.23 (t, *J* = 10 Hz, 1H). **^{13}C NMR (MeOD-*d*$_3$:CDCl$_3$, 500 MHz, calibrated to residual MeOH peak, 49.00 ppm)** δ 24.1, 106.9, 108.7, 113.1, 114.0, 133.1, 148.9, 156.6, 156.8, 163.3. **HRMS (FAB+):** calculated for $C_{10}H_{10}NO_2$ 176.0712, measured 176.0710 [M+1].

***tert*-butyl 4-(4-methyl-2-oxo-2*H*-chromen-7-yl)piperazine-1-carboxylate (25)** was eluted with 30% EtOAc:Hex as a white solid (isolated as a 4.8:1 mixture of **25:26** with [Pt] 45 mg, 66%. Isolated as a 5.5:1 mixture of **25:26** with [Au] 55 mg, 80%). **^{1}H NMR ($CDCl_3$, 400 MHz)** δ 1.49 (s, 9H); 2.37 (s, 3H); 3.31 (t, *J* = 4.8 Hz, 4H); 3.60 (t, *J* = 4.8 Hz, 4H); 6.05 (s, 1H); 6.70 (d, *J* = 2.4 Hz, 1H); 6.82 (dd, *J* = 8.8 Hz, *J* = 2.4 Hz, 1H); 7.45 (d, *J* = 8.8 Hz, 1H); **^{13}C NMR ($CDCl_3$, 100 MHz)** δ 18.6, 28.5, 47.6, 80.2, 101.6, 111.0, 111.7, 111.9, 125.5, 152.6, 153.4, 154.6, 155.4, 161.7. **HRMS (FAB+):** calculated for $C_{19}H_{24}N_2O_4$ 344.1736, measured 344.1743 [M].

***tert*-butyl 4-(4-methyl-2-oxo-2*H*-chromen-5-yl)piperazine-1-carboxylate (26)** was eluted with 30% EtOAc:Hex as an amorphous white solid (isolated as a 4.8:1 mixture of **25:26** with [Pt] 45 mg, 66%. Isolated as a 5.5:1 mixture of **25:26** with [Au] 55 mg, 80%). **^{1}H NMR ($CDCl_3$, 400 MHz)** δ 1.49 (s, 9H); 2.76 (s, 3H); 2.85-2.79 (m, 2H); 3.00 (d, *J* = 11.2 Hz, 2H); 3.13 (bs, 2H); 4.11 (bs, 2H); 6.19 (d, *J* = 0.8 Hz, 1H); 7.09 (dd, *J* = 8.0 Hz, *J* = 1.2 Hz, 1H); 7.14 (dd, *J* = 8.4 Hz, *J* = 0.8 Hz, 1H); 7.46 (t, *J* = 8.4 Hz, 1H); **^{13}C NMR ($CDCl_3$, 100 MHz)** δ 23.8, 28.5, 54.1, 80.2, 114.3, 116.0, 116.4, 117.6, 131.6, 152.5, 153.6, 154.8, 155.4, 160.4. **HRMS (FAB+):** calculated for $C_{19}H_{24}N_2O_4$ 344.1736, measured 344.1743 [M].

2,3,6,7-tetrahydro-9-methyl-*1H,5H,11H*-[1]benzopyrano[6,7,8-ij]quinolizin-11-one (28) was eluted with 20% EtOAc:Hex as an amorphous yellow solid (45 mg, 88% with [Pt]; 47 mg, 91% with [Au]). **^{1}H NMR ($CDCl_3$, 400 MHz)** δ 2.00-1.93 (m, 4H); 2.30 (s, 3H); 2.77 (t, *J* = 6.0 Hz, 2H); 2.87 (t, *J* = 6.4 Hz, 2H); 3.27-3.21 (m, 4H); 5.88 (s, 1H); 6.97 (s, 1H); **^{13}C NMR ($CDCl_3$, 100 MHz)** δ 18.6, 20.5, 20.7, 21.6, 27.8, 49.5, 50.0, 106.7, 108.1, 108.9, 118.0, 121.7, 145.8, 151.0, 153.1, 162.6. **HRMS (FAB+):** calculated for $C_{16}H_{17}NO_2$ 255.1259, measured 255.1255 [M].

4-methyl-pyrano[2,3-*a*]carbazol-2(5H)-one (30) was eluted with 50% EtOAc:Hex as an amorphous pale yellow solid (isolated as a 5:1 mixture of **30:31** with [Pt] 69 mg, 69%. Isolated as a 1.7:1 mixture of 30:31 with [Au] 92 mg, 92%). **^{1}H NMR (DMSO-d_6, 400 MHz)** δ 2.86 (s, 3H); 6.35 (s, 1H); 7.19 (d, *J* = 8.4 Hz, 1H); 7.24 (t, *J* = 7.6 Hz, 1H); 7.43 (dt, *J* = 8.0 Hz, *J* = 0.8 Hz, 1H); 7.71 (d, *J* = 8.4 Hz, 1H); 8.16 (d, *J* = 7.6 Hz, 1H); 8.36 (d, *J* = 8.4 Hz, 1H); 11.14 (s, 1H); **^{13}C NMR (DMSO-d_6, 100 MHz)** δ 22.6, 106.0, 108.4, 112.2, 112.6, 119.6, 119.8, 119.9, 121.6, 124.1, 125.4, 135.0, 140.3, 152.9, 153.0, 159.9. **HRMS (FAB+):** calculated for $C_{16}H_{12}NO_2$ 250.0868, measured 250.0864 [M+1].

4-methyl-pyrano[2,3-*b*]carbazol-2(10H)-one (31) was eluted with 30% EtOAc:Hex as an amorphous white solid (isolated as a 5:1 mixture of **30:31** with [Pt] 69 mg, 69%. Isolated as a 1.7:1 mixture of **30:31** with [Au] 92 mg, 92%). **^{1}H NMR (DMSO-d_6, 400 MHz)** δ 2.56 (s, 3H); 6.23 (d, *J* = 1.2 Hz, 1H); 7.23 (dt, *J* = 7.6 Hz, *J* = 0.8 Hz, 1H); 7.38 (s, 1H); 7.43 (dt, *J* = 8.0 Hz, *J* = 1.2 Hz, 1H); 7.51 (d, *J* = 8.0 Hz, 1H); 8.23 (d, *J* = 8.0 Hz, 1H); 8.55 (s, 1H); 11.63 (s, 1H); **^{13}C NMR (DMSO-d_6, 100 MHz)** 18.7, 97.2, 110.5, 111.2, 112.5, 117.2, 119.5, 120.3, 120.6, 122.2, 126.3, 140.9, 142.0, 152.1, 154.3, 160.5. **HRMS (FAB+):** calculated for $C_{16}H_{12}NO_2$ 250.0868, measured 250.0864 [M+1].

2,3,6,7-tetrahydro-9-(ethyl-2-*tert*-butoxycarbonylamino)-*1H,5H,11H*-[1]benzopyrano[6,7,8-*ij*]quinolizin-11-one (35) was eluted with 30% EtOAc/Hex as an amorphous pale yellow solid (229 mg, 91% with [Pt]; 73 mg, 95% with [Au]). **^{1}H NMR ($CDCl_3$, 300 MHz)** δ 1.44 (s, 9H); 1.97 (quint, *J* = 6.3 Hz, 4H); 2.78 (t, *J* = 6.6 Hz, 2H); 2.91-2.83 (m, 4H); 3.25 (quart, *J* = 6.0 Hz, 4H); 3.43 (q, *J* = 6.3 Hz, 2H); 4.64 (br s, 1H); 5.89 (s, 1H); 7.04 (s, 1H); **^{13}C NMR ($CDCl_3$, 75 MHz)** δ 20.6, 20.8, 21.7, 28.0, 28.5, 32.4, 39.8, 49.6, 50.0, 79.7, 107.0, 107.9, 118.3, 121.6, 146.0, 151.5, 154.0, 155.9, 162.4. **HRMS (FAB+):** calculated for $C_{22}H_{28}N_2O_4$ 384.2049, measured 384.2048 [M].

2,3,6,7-tetrahydro-9-(propyl-2-*tert*-butoxycarbonylamino)-*1H*,*5H*,*11H*-[1]benzopyrano[6,7,8-*ij*]quinolizin-11-one (37) was eluted with 20% EtOAc/Hex as an amorphous pale yellow solid (70 mg, 88% with [Pt]; 72 mg, 90% with [Au]). **^{1}H NMR ($CDCl_3$, 400 MHz)** δ 1.15 (d, *J* = 6.4 Hz, 3H); 1.44 (s, 9H); 1.98-1.96 (br m, 4H); 2.58-2.53 (m, 1H); 2.80 (t, *J* = 6.0 Hz, 2H); 2.88 (t, *J* = 6.4 Hz, 2H); 3.03 (br s, 1H); 3.28-3.23 (br m, 4H); 4.01-3.97 (m, 1H); 4.47 (br s, 1H); 5.87 (s, 1H); 7.27 (s, 1H, overlaps with residual solvent peak); **^{13}C NMR ($CDCl_3$, 75 MHz)** δ. 20.6, 20.8, 21.7, 27.9, 28.5, 40.0, 46.2, 49.6, 50.1, 79.5, 106.9, 108.3, 108.8, 118.3, 122.2, 146.0, 151.5, 153.5, 155.2, 162.5. **HRMS (FAB+):** calculated for $C_{23}H_{30}N_2O_4$ 398.2206, measured 398.2193 [M].

2,3,6,7-tetrahydro-9-(methyl-*tert*-butoxycarbonylamino)-*1H*,*5H*,*11H*-[1]benzopyrano[6,7,8-*ij*]quinolizin-11-one (39) was eluted with 30% EtOAc/Hex as an amorphous pale yellow solid (65 mg, 88% with [Pt]; 67 mg, 90% with [Au]). **^{1}H NMR ($CDCl_3$, 300 MHz)** δ 1.47 (s, 9H); 1.96 (quint, *J* = 6.3 Hz, 4H); 2.75 (t, *J* = 6.6 Hz, 2H); 2.87 (t, *J* = 6.6 Hz, 2H); 3.25 (quart, *J* = 5.7 Hz, 4H); 4.40 (d, *J* = 6.0 Hz, 2H); 4.84 (br s, 1H); 6.01 (s, 1H); 6.98 (s, 1H); **^{13}C NMR ($CDCl_3$, 75 MHz)** δ 20.6, 20.8, 21.7, 27.9, 28.5, 41.0, 49.7, 50.1, 80.4, 105.7, 106.8, 107.1, 118.3, 120.9, 146.1, 151.4, 152.9, 155.7, 162.6. **HRMS (FAB+):** calculated for $C_{21}H_{26}N_2O_4$ 370.1893, measured 370.1879 [M]

6,7,8,9-tetrahydro-2-oxo-4-(ethyl-*tert*-butoxycarbonylamino)-9-(2-propen-1-yl)-*2H*-pyrano[3,2-*g*]quinoline (41) was eluted with 30% EtOAc/Hex as an amorphous pale yellow solid (290 mg, 76% with [Pt]; 72 mg, 93% with [Au]). **^{1}H NMR ($CDCl_3$, 400 MHz)** δ 1.45 (s, 9H); 1.98 (quint, *J* = 6.0 Hz, 2H); 2.80 (t, *J* = 6.0 Hz, 2H); 2.87 (t, *J* = 6.8 Hz, 2H); 3.38 (t, *J* = 6.8 Hz, 2H); 3.46-3.42 (m, 2H); 3.91 (dd, *J* = 2.8 Hz, *J* = 2.0 Hz, 2H); 4.66 (br s, 1H) 5.21-5.14 (m, 2H); 5.84-5.76 (m, 1H); 5.90 (s, 1H); 6.40 (s, 1H); 7.16 (s, 1H); **^{13}C NMR ($CDCl_3$, 100 MHz)** δ 22.0, 28.0, 28.5, 32.4, 39.7, 49.2, 53.8, 79.7, 97.4, 108.2, 108.5, 116.7, 119.7, 123.8, 131.5, 148.6, 153.7, 155.2, 155.9, 162.2. **HRMS (FAB+):** calculated for $C_{22}H_{28}N_2O_4$ 384.2049, measured 384.2046 [M].

6,7,8,9-tetrahydro-2-oxo-4-(propyl-2-*tert*-butoxycarbonylamino)-9-(2-propen-1-yl)-*2H*-pyrano[3,2-*g*]quinoline (43) was eluted with 20% EtOAc/Hex as an amorphous pale yellow solid (60 mg, 75% with [Pt]; 73 mg, 92% with [Au]). **^{1}H NMR ($CDCl_3$, 400 MHz)** δ 1.13 (d, *J* = 6.8 Hz, 3H); 1.40 (s, 9H); 1.94 (quint, *J* = 5.6 Hz, 2H); 2.55-2.50 (m, 1H); 2.79 (t, *J* = 6.0 Hz, 2H); 3.03-3.01 (m, 1H); 3.34 (t, *J* = 6.0 Hz, 2H); 3.86 (d, *J* = 4.4 Hz, 2H) 3.96 (quint, *J* = 6.8 Hz, 1H); 4.61 (br s, 1H); 5.17-5.10 (m, 2H); 5.81-5.72 (m, 1H); 5.85 (s, 1H); 6.34 (s, 1H); 7.36 (s, 1H); **^{13}C NMR ($CDCl_3$, 100 MHz)** δ 20.4, 21.9, 27.9, 28.4, 39.9, 46.0, 49.2, 53.7, 79.4, 97.1, 108.4, 109.2, 116.5, 119.6, 124.4, 131.5, 148.4, 153.3, 155.0, 155.2, 162.2. **HRMS (FAB+):** calculated for $C_{23}H_{30}N_2O_4$ 398.2206, measured 398.2215 [M].

7,8,9,10-tetrahydro-2-oxo-4-(ethyl-*tert*-butoxycarbonylamino)-7-(2-propen-1-yl)-*2H*-pyrano[3,2-*f*]quinoline (45) was eluted with 20% EtOAc/Hex as an amorphous pale yellow solid (71 mg, 74% with [Pt]; 86 mg, 90% with [Au]). **^{1}H NMR ($CDCl_3$, 400 MHz)** δ 1.44 (s, 9H); 2.05-1.95 (m, 2H); 2.92-2.87 (m, 4H); 3.42-3.34 (m, 4H); 3.97-3.95 (m, 2H); 4.85 (s, 1H); 5.19-5.14 (m, 2H); 5.87-5.78 (m, 1H); 5.92 (s, 1H); 6.52 (d, *J* = 9.2 Hz, 1H); 7.36 (d, *J* = 8.8 Hz, 1H); **^{13}C NMR ($CDCl_3$, 100 MHz)** δ 20.6, 21.0, 28.4, 32.5, 39.9, 49.0, 53.9, 79.6, 108.0, 108.3, 108.5, 116.4, 123.0, 132.2, 148.4, 152.5, 154.2, 155.9, 162.3. **HRMS (FAB+):** calculated for $C_{22}H_{24}N_2O_4$ 384.2049, measured 384.2041 [M].

7,8,9,10-tetrahydro-2-oxo-4-(ethyl-*tert*-butoxycarbonylamino)-*2H*-pyrano[3,2-*f*]quinoline (PV139)—To an oven dried vial was added **7,8,9,10-tetrahydro-2-oxo-4-(ethyl-*tert*-butoxycarbonylamino)-7-(2-propen-1-yl)-*2H*-pyrano[3,2-*f*]quinoline (45)** (306 mg, 0.79 mmol) followed by THF (18 mL). To the resulting solution was added *N,N′*-dimethylbarbituric acid (370 mg, 2.37 mmol) and $Pd(PPh_3)_4$ (92 mg, 0.079 mmol, 10 mol

%). The mixture was then sealed with a Teflon screw-cap under an atmosphere of argon and heated to 80 °C for 12 hr. Upon consumption of the starting material, the reaction mixture was concentrated and the resulting residue was purified by flash column chromatography (eluting with 30% EtOAc/Hex) to afford **7,8,9,10-tetrahydro-2-oxo-4-(ethyl-*tert*-butoxycarbonylamino)-*2H*-pyrano[3,2-*f*]quinoline** (250 mg, 0.73 mmol) as an amorphous yellow solid, 92%. **^{1}H NMR ($CDCl_3$, 400 MHz)** δ 1.44 (s, 9H); 1.95-1.92 (m, 2H); 2.87-2.85 (m, 4H); 3.41-3.33 (m, 4H); 4.64 (br s, 1H); 4.87 (br s, 1H); 5.92 (s, 1H); 6.39 (d, *J* = 8.4 Hz, 1H); 7.28 (d, *J* = 9.2 Hz, 1H); **^{13}C NMR ($CDCl_3$, 100 MHz)** δ 20.0, 20.7, 28.4, 32.6, 39.9, 41.2, 79.6, 107.3, 108.2, 109.1, 111.0, 122.8, 148.5, 153.2, 154.4, 155.9, 162.2. This material (222 mg, 0.65 mmol) in DCM (3.75 mL) was added TFA (1.20 mL) slowly at 0 °C. The reaction stirred for 15 min at 0 °C at which time the starting material had been fully consumed. The solvent was removed *in vacuo* and the residue was purified via HPLC eluting with MeCN:H_2O (the water contained 1% TFA). The fractions containing the product were pooled and evaporated. The residue was then lyophilized to afford **7,8,9,10-tetrahydro-2-oxo-4-(2-aminoethyl)-*2H*-pyrano[3,2-*f*]quinoline (PV139 TFA salt)** as an amorphous yellow solid (130 mg, 0.36 mmol, 55%). **^{1}H NMR (CD_3OD, 400 MHz)** δ 1.90 (quint, *J* = 8.4 Hz, 2H); 2.79 (t, *J* = 8.4 Hz, 2H); 3.06 (t, *J* = 9.6 Hz, 2H); 3.32-3.22 (m, 4H); 5.93 (s, 1H); 6.52 (d, *J* = 12.0 Hz, 1H); 7.31 (d, *J* = 11.6 Hz, 1H); **^{13}C NMR (CD_3OD, 75 MHz)** δ 20.0, 20.5, 29.5, 38.6, 40.7, 106.4, 106.8, 107.9, 111.6, 122.7, 150.2, 153.4, 153.5, 163.3. **^{19}F-NMR ($CDCl_3$, 300 MHz)** δ −76.51. **HRMS (FAB+):** calculated for $C_{14}H_{17}N_2O_2$ 245.1290, measured 245.1283 [M – trifluoroacetate].

9-(2-aminoethyl)-2,3,6,7-tetrahydro-*1H*,*5H*,*11H*-[1]benzopyrano[6,7,8-*ij*]quinolizin-11-one (FFN511 TFA salt)—To a solution of **2,3,6,7-tetrahydro-9-(ethyl-2-*tert*-butoxycarbonylamino)-*1H*,*5H*,*11H*-[1]benzopyrano[6,7,8-*ij*]quinolizin-11-one (35)** (177 mg, 0.46 mmol) in DCM (6 mL) was added TFA (2 mL) slowly at 0 °C. The reaction stirred for 10 min at 0 °C at which time the starting material had been fully consumed. The solvent was removed *in vacuo* and the residue was quenched with satd. $NaHCO_3$ (aq.) (~20 mL). The resulting solution was extracted with 10% MeOH/$CHCl_3$ (6 × 10 mL). The organic layers were combined and dried over $MgSO_4$. The solvent was removed *in vacuo* and the resulting residue was purified via HPLC eluting with MeCN:H_2O (the water contained 1% TFA). The fractions containing the product were pooled and evaporated. The residue was then lyophilized to afford **9-(2-aminoethyl)-2,3,6,7-tetrahydro-*1H*,*5H*,*11H*-[1]benzopyrano[6,7,8-*ij*]quinolizin-11-one (FFN511 TFA salt)** as an amorphous yellow solid (151 mg, 0.38 mmol, 82%). **^{1}H NMR (CD_3OD, 300 MHz)** δ 1.99-1.95 (m, 4H); 2.82 (apparent quart, *J* = 6.6 Hz, 4H); 3.06 (t, *J* = 6.5 Hz, 2H); 3.25 (t, *J* = 7.8 Hz, 2H); 3.33 (eclipsed by solvent, 4H); 5.93 (s, 1H); 7.16 (s, 1H); **^{13}C NMR ($CDCl_3$, 75 MHz)** δ 20.6, 20.7, 21.7, 27.8, 36.0, 41.4, 49.6, 50.0, 107.1, 107.8, 108.0, 118.1, 121.5, 145.9, 151.5, 154.4, 162.5. **^{19}F NMR ($CDCl_3$, 300 MHz)** δ −76.38. **HRMS (FAB+):** calculated for $C_{17}H_{21}N_2O_2$ 285.1603, measured 285.1601 [M – trifluoroacetate].

9-(2-aminoethyl)-2,3,6,7-tetrahydro-*1H*,*5H*,*11H*-[1]benzopyrano[6,7,8-*ij*]quinolizin-11-one (FFN511)—A solution of **FFN511 TFA salt** (110 mg, 0.27 mmol) in H_2O (8 mL) was prepared; slight warming was required to fully dissolve all solids. To the resulting solution was added satd. $NaHCO_3$ (aq.) (~10 mL). The solution was extracted with 10% MeOH/$CHCl_3$ (10 × 10 mL). The organic layers were combined and dried over $MgSO_4$. The solvent volume was reduced on a rotary evaporator at which point the product began to crystallize. The remaining solution was allowed to evaporate slowly to afford product **9-(2-aminoethyl)-2,3,6,7-tetrahydro-*1H*,*5H*,*11H*-[1]benzopyrano[6,7,8-*ij*]quinolizin-11-one (FFN511)** (74 mg, 0.26 mmol) yellow crystals, 96%. **^{1}H NMR ($CDCl_3$, 300 MHz)** δ 1.38 (br s, 2H); 1.97 (quint, *J* = 6.3 Hz, 4H); 2.79 (quart, *J* = 6.6 Hz, 4H); 2.89 (t, *J* = 6.6 Hz, 2H); 3.04 (t, *J* = 6.6 Hz, 2H); 3.25 (quart, *J* = 6.3 Hz, 4H); 5.92 (s,

1H); 7.02 (s, 1H); **^{13}C NMR ($CDCl_3$, 75 MHz)** δ 20.6, 20.7, 21.5, 27.8, 35.9, 41.4, 49.5, 49.9, 106.9, 107.6, 107.9, 118.1, 121.5, 145.8, 151.4, 154.4, 162.4. **HRMS (FAB+):** calculated for $C_{17}H_{21}N_2O_2$ 285.1603, measured 285.1601 [M+1]. **Melting point:** 160.9–162.1 °C.

Supplementary Material

Refer to Web version on PubMed Central for supplementary material.

Acknowledgments

This work was supported by the National Institute of Mental Health (MH086545) and the G. Harold & Leila Y. Mathers Charitable Foundation. We would also like to thank the Parkin research group for X-ray crystal analysis. The National Science Foundation (CHE-0619638) is thanked for acquisition of an X-ray diffractometer.

References

1. (a) Godula K, Sames D. Science. 2006; 312:67–72. [PubMed: 16601184] (b) Kakiuchi F, Chatani N. Adv Synth Catal. 2003; 345:1077–1101.
2. Kitamura T. Eur J Org Chem. 2009:1111–1125.
3. (a) Pastine SJ, Youn SW, Sames D. Org Lett. 2003; 5:1055–1058. [PubMed: 12659572] (b) Pastine SJ, Youn SW, Sames D. Tetrahedron. 2003; 59:8859–8868.(c) Pastine SJ, Sames D. Org Lett. 2003; 5:4053–4055. [PubMed: 14572247]
4. Youn SW, Pastine SJ, Sames D. Org Lett. 2004; 6:581–584. [PubMed: 14961628]
5. Milder conditions for the von Pechmann condensation using Lewis acid promoters has been demonstrated with hydroxyjulolidine. Wirtz L, Kazmaier U. Eur J Org Chem. 2011:7062.
6. Chen G, Yee DJ, Gubernator NG, Sames D. J Am Chem Soc. 2005; 127:4544–4545. [PubMed: 15796498]
7. (a) Wise RA. Nature Rev Neurosci. 2004; 5:1–12.(b) Bamford NS, Zhang H, Schmitz Y, Wu NP, Cepeda C, Levine MS, Schmauss C, Zakharenko SS, Zablow L, Sulzer D. Neuron. 2004; 42:653–663. [PubMed: 15157425]
8. Verhoeff NPLG. Neuropsychopharm. 1999; 147:217–249.
9. Gubernator NG, Zhang H, Staal RGW, Mosharov EV, Pereira DB, Yue M, Balsanek V, Vadola PA, Mukherjee B, Edwards RH, Sulzer D, Sames D. Science. 2009; 324:1441–1444. [PubMed: 19423778]
10. Schimitschek EJ, Trias JA, Hammond RA, Atkins H, Atkins RL. Optics Commun. 1976; 16:313.
11. (a) Jia C, Piao D, Oyamada J, Lu W, Kitamura T, Fujiwara Y. Science. 2000; 287:1992–1995. [PubMed: 10720319] (b) Jia C, Lu W, Oyamada J, Kitamura T, Matsuda K, Irie M, Fujiwara Y. J Am Chem Soc. 2000; 122:7252–7263.(c) Jia C, Piao D, Kitamura T, Fujiwara Y. J Org Chem. 2000; 65:7516–7522. [PubMed: 11076610] (d) Kitamura T, Otsubo K. J Org Chem. 2012; 77:2978–2982. [PubMed: 22372387]
12. Martín-Matute B, Nevado C, Cárdenas DJ, Echavarren AM. J Am Chem Soc. 2003; 125:5757–5766. [PubMed: 12733916]
13. (a) Fürstner A, Mamane V. J Org Chem. 2002; 67:6261–6267.(b) Mamane V, Hannen P, Fürstner A. Chem Eur J. 2004; 10:4556–4575. [PubMed: 15378635]
14. Reetz MT, Sommer K. Eur J Org Chem. 2003:3485–3496.
15. (a) Fürstner A. Chem Soc Rev. 2009; 38:3208–3221. [PubMed: 19847352] (b) Fürstner A, Davies PW. Angew Chem Int Ed. 2007; 46:3410–3449.
16. (a) Ferrer C, Echavarren AM. Angew Chem, Int Ed. 2006; 45:1105–1109.(b) Nevado C, Echavarren AM. Chem Eur J. 2005; 11:3155–3164. [PubMed: 15779093]
17. Gorin DJ, Toste FD. Nature. 2007; 446:395–403. [PubMed: 17377576]
18. Shi Z, He C. J Org Chem. 2004; 69:3669–3671. [PubMed: 15152995]
19. Dang TT, Boeck F, Hintermann L. J Org Chem. 2011; 76:9353–9361. [PubMed: 22010906]

20. Huang Z, McGowan EB, Detwiler TC. J Med Chem. 1992; 35:2048–2054. [PubMed: 1597856]
21. Beaulieu PL, Bös M, Bousquet Y, DeRoy P, Fazal G, Gauthier J, Gillard J, Goulet S, McKercr G, Poupart MA, Valois S, Kukolj G. Bioorg Med Chem Lett. 2004; 14:967–971. [PubMed: 15013003]
22. Becker MH, Chua P, Downham R, Douglas CJ, Garg NK, Hiebert S, Jaroch S, Matsuoka RT, Middleton JA, Ng FW, Overman LE. J Am Chem Soc. 2007; 129:11987–12002. [PubMed: 17850086]

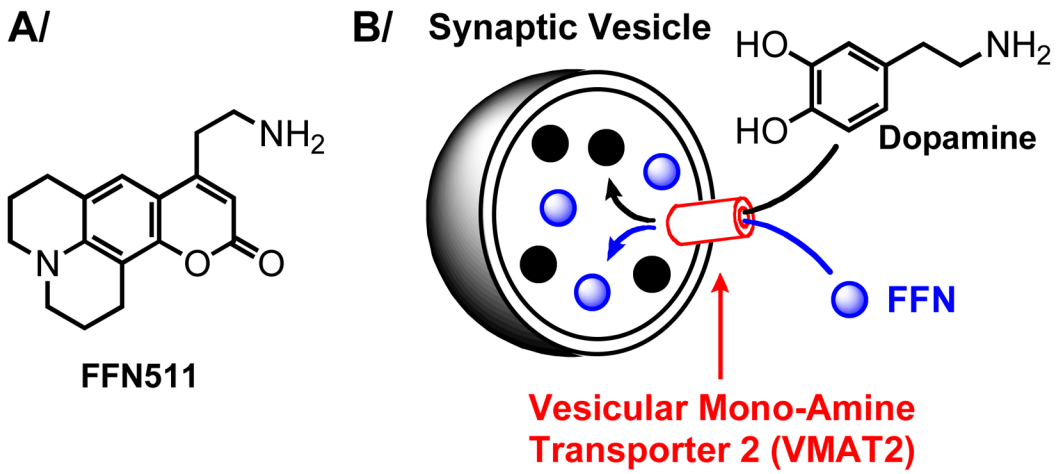

Figure 1.

Fluorescent False Neurotransmitters (FFNs) were recently introduced to enable optical imaging of neurotransmission at individual synapses in the brain. A) The structure of the first example of FFNs, compound FFN511. B) FFNs function as fluorescent substrates of vesicular monoamine transporter 2 (VMAT2), the protein that accumulates dopamine in synaptic vesicles. In this manner, FFNs act as optical tracers of the neurotransmitter, allowing for imaging of both location (accumulation of fluorescence signal) and activity of presynaptic terminals (loss of fluorescence signal).

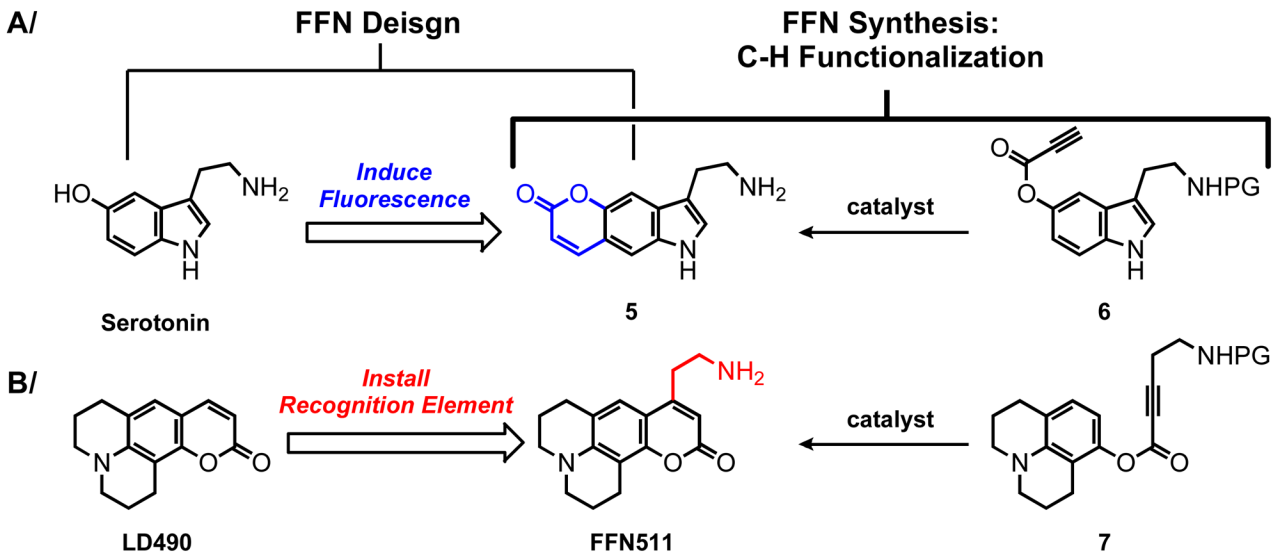

Figure 2.

Two design approaches to Fluorescent False Neurotransmitters (FFNs). (A) A monoamine neurotransmiter such as serotonin is modified by addition of the lactone ring to render the system fluorescent (fluorescent pyrrolocoumarin **5)**. (B) A known fluorophore (in this case **LD490**) is elaborated to include the ethylamino group, which is the key recognition element for the relevant monoamine transporter VMAT2, providing the probe **FFN511**.

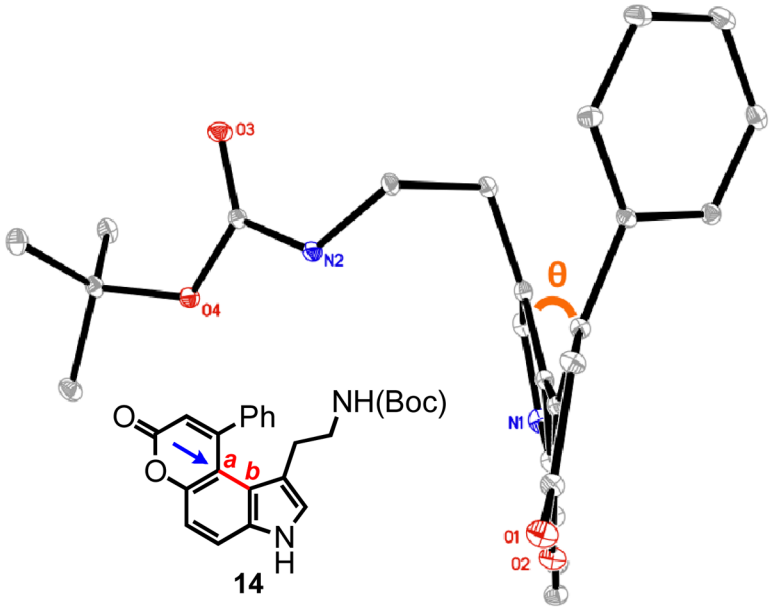

Figure 3.
ORTEP plot of the X-ray structure of compound **14**. The dihedral angle of 19.4° is labeled as θ. ORTEP graphic is oriented to see down the C_a-C_b bond.

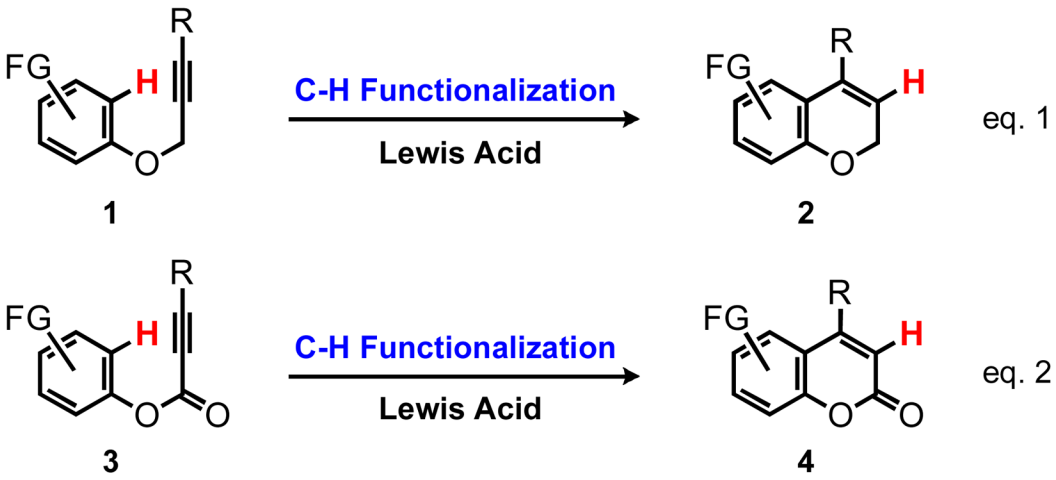

Scheme 1.
Selective 6-endo Annulation via Hydroarylation

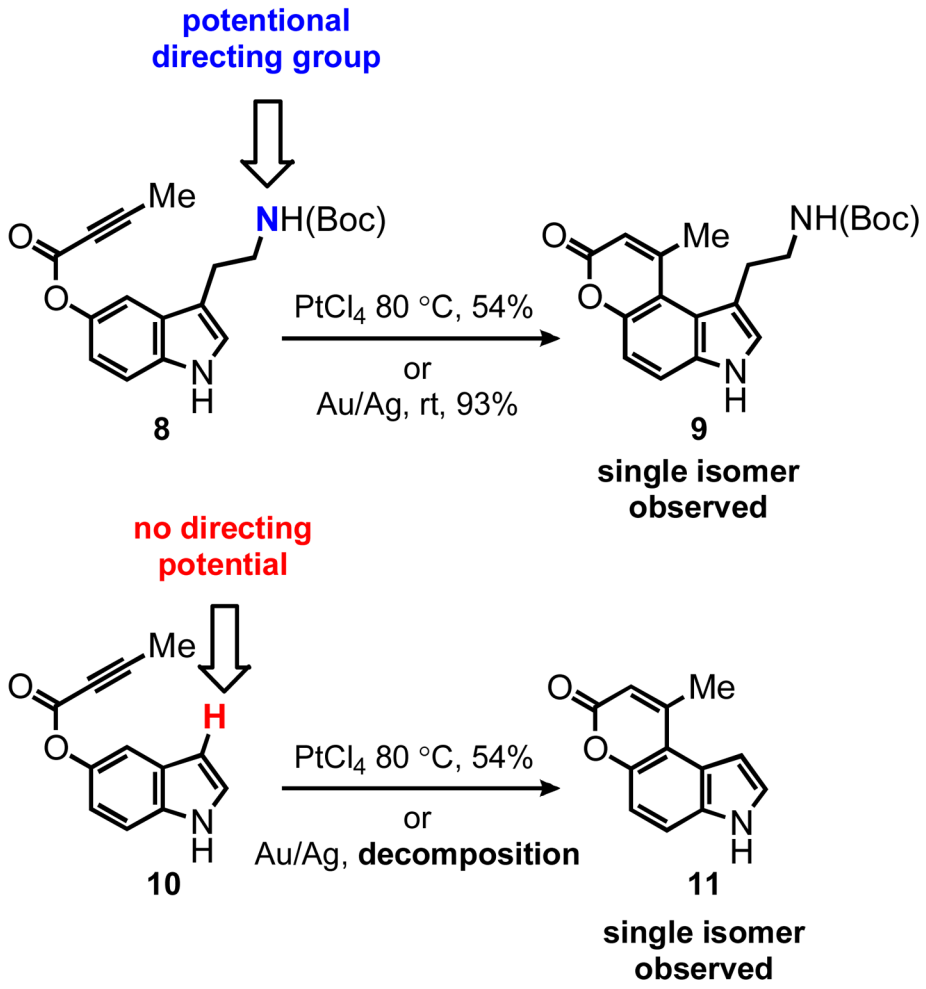

Scheme 2.
The cyclization is not directed by the substituent in 3-position

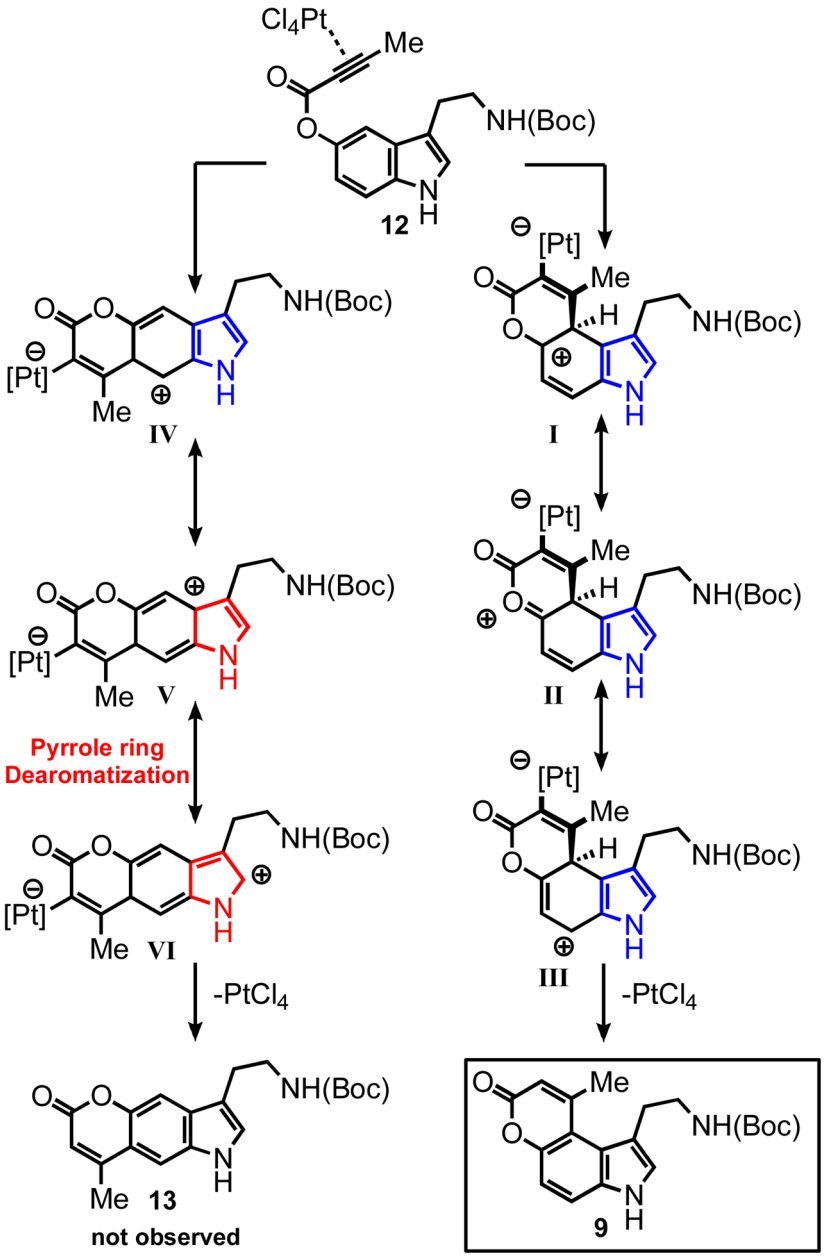

Scheme 3.
Mechanistic rationale for the observed regioselectivity in the cyclization of indole substrates

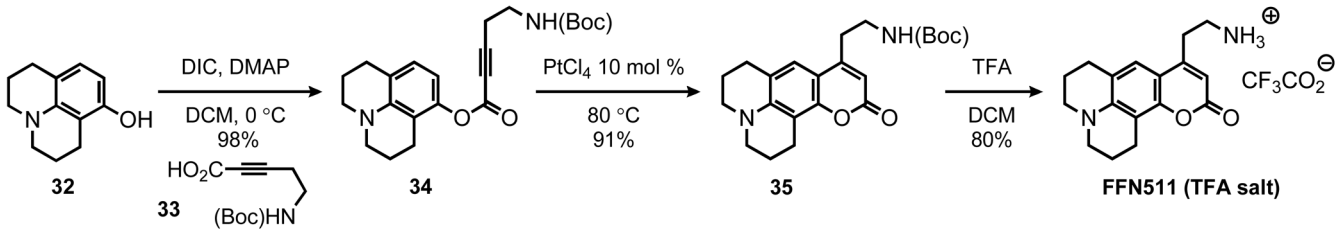

Scheme 4.
Synthesis of FFN511 via the Catalytic Hydroarylation

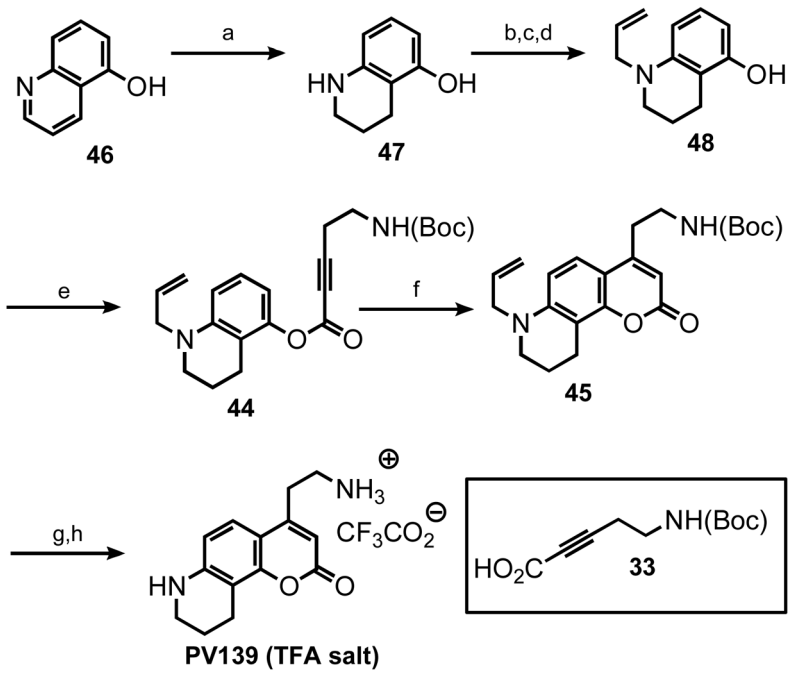

Scheme 5.

Synthesis of a new FFN candidate, compound **PV139**

a) H_2 (3 atm), PtO_2 EtOH, HCl (aq.), 69%. b) TBSCl, imidazole, DMF 50 °C. c) allylbromide, K_2CO_3, MeCN, 100 °C. d) TBAF, THF; 65% for 3 steps. e) **33**, DIC, DMAP, DCM, 0 °C, 70%. f) see Table 5. g) $Pd(PPh_3)_4$ (5 mol %), *N,N′*-dimethylbarbituric acid, THF, 80 °C. h) TFA, DCM, 0 °C; 90% for 2 steps.

Table 1

Comparing $PtCl_4$ Against Known Platinum and Palladium Catalytic Systems

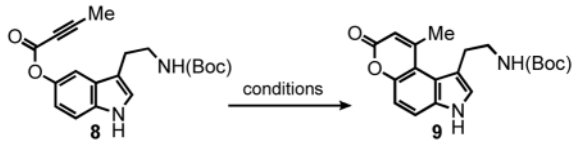

entry	catalyst	mol %	solvent[a]	yield 9	recov. 8
1[b]	$PtCl_4$	10	DCE:dioxane	54	0
2[b]	$PtCl_4$	5	DCE:dioxane	31	51
3[c]	$Pd(OAc)_2$	5	TFA:DCM	0	0
4[b]	$PtCl_2$	5	Toluene	50	13
5[d]	$PtCl_2$	5	Dioxane	32	14
6[d]	$PtCl_2$	5	Acetone	4	60

[a] all reactions were run at a concentration of 0.05M.

[b] entries 1, 2 and 4 were run at 80 °C.

[c] entry 3 was run at room temperature.

[d] entries 5 and 6 were heated to reflux.

Table 2

Optimization $Au(PPh_3)Cl/AgSbF_6$ Catalyst Loading[a]

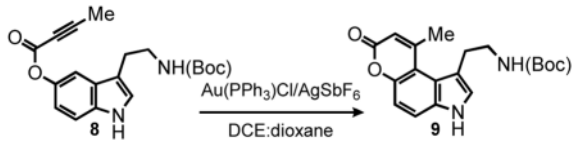

entry	mol %	temp. °C	time	yield 9
1	10	23	<5 min	92
2	5	23	<10 min	94
3	2	80	1 hr	94
4	1	80	6 hr	93

[a]All reactions were run at a concentration of 0.05M.

Table 3

Scope Summary of Indole Derived Aryl Alkynoate Ester Substrates

entry	substrate	product	conditions/yield	
1	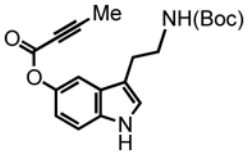 **8**	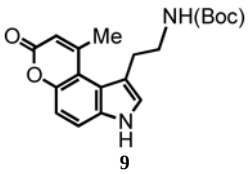 **9**	Pt, 80 °C Au, r.t.	**54%** **93%**
2	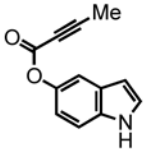 **10**	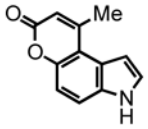 **11**	Pt, 80 °C Au	**54%** **decomp.**
3	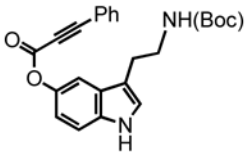 **15**	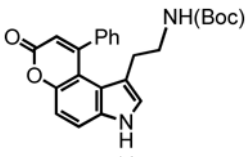 **14**	Pt Au, r.t.	**N.R.** **98%**
4	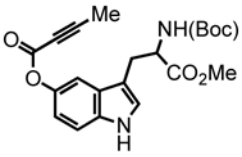 **16**	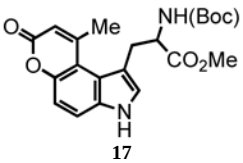 **17**	Pt, 80 °C Au, r.t.	**50%** **80%**

Table 4

Exploring the Scope of Aniline Substrates

entry	substrate	product	conditions/yield
1	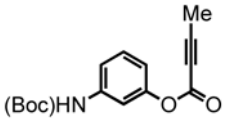 **18**	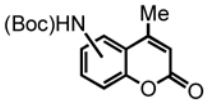 7-NH(Boc)-**19** 5-NH(Boc)-**20**	Pt **N.R.** Au, r.t. **86%** **19:20** = 3.5:1
2	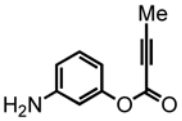 **21**	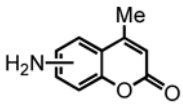 7-NH_2-**22** 5-NH_2-**20**	Pt **N.R.** Au, r.t. **95%** **22:23** = 1:1
3	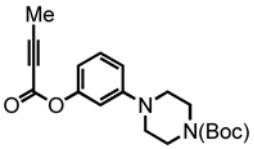 **24**	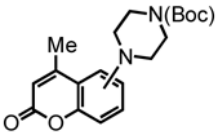 7-NH(Boc)-**25** 5-NH(Boc)-**26**	Pt, 80 °C **66%** **25:26** = 4.8:1 Au, 80 °C **80%** **25:26** = 5.5:1
4	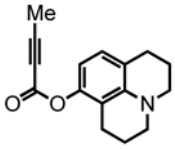 **27**	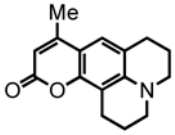 **28**	Pt, 80 °C **88%** Au, r.t. **91%**
5	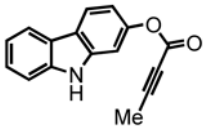 **29**	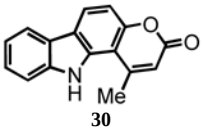 **30** 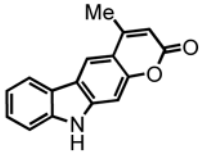 **31**	Pt, 80 °C **69%** **30:31** = 5:1 Au, r.t **92%** **30:31** = 1.7:1

Table 5

Complex Aryl Alkynoate Esters as Precursors to New FFN Probes

entry	substrate	product	conditions/yield	
1	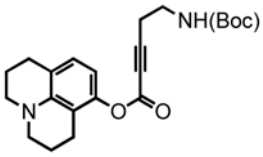 **34**	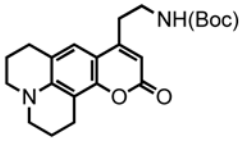 **35**	Pt, 80 °C Au/Ag, r.t.	**91%** **95%**
2	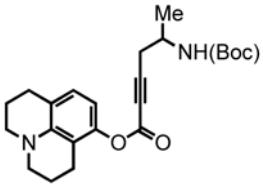 **36**	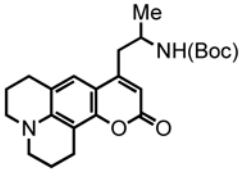 **37**	Pt, 80 °C Au/Ag, r.t.	**88%** **90%**
3	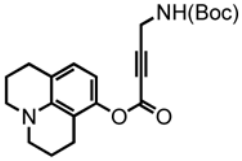 **38**	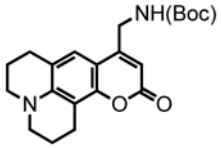 **39**	Pt, 80 °C Au/Ag, r.t.	**88%** **90%**
4	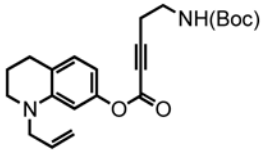 **40**	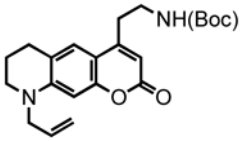 **41**	Pt, 80 °C Au/Ag, r.t.	**76%** **93%**
5	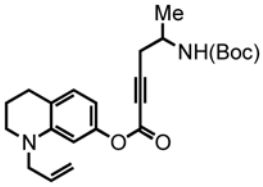 **42**	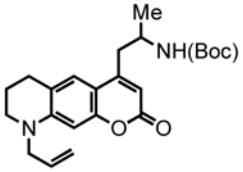 **43**	Pt, 80 °C Au/Ag, r.t.	**75%** **92%**
6	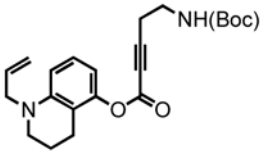 **44**	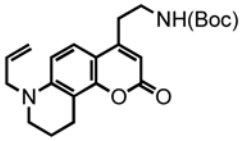 **45**	Pt, 80 °C Au/Ag, r.t.	**74%** **90%**